

ภาวะแก้วสปีนในแบบจำลองไอซิงที่มีพันธะแบบสุ่ม



นายลือชา ตั้งชนะชัยอนันต์

ศูนย์วิทยทรัพยากร  
จุฬาลงกรณ์มหาวิทยาลัย

วิทยานิพนธ์ฉบับนี้เป็นส่วนหนึ่งของการศึกษาตามหลักสูตรปริญญาวิทยาศาสตรมหาบัณฑิต

สาขาวิชาฟิสิกส์ ภาควิชาฟิสิกส์

คณะวิทยาศาสตร์ จุฬาลงกรณ์มหาวิทยาลัย

ปีการศึกษา 2552

ลิขสิทธิ์ของจุฬาลงกรณ์มหาวิทยาลัย

SPIN GLASS PHASE IN RANDOM-BOND ISING MODEL



Mr. Luecha Tungchanachaiyanun

ศูนย์วิทยทรัพยากร  
จุฬาลงกรณ์มหาวิทยาลัย

A Thesis Submitted in Partial Fulfillment of the Requirements  
for the Degree of Master of Science Program in Physics

Department of Physics

Faculty of Science


Chulalongkorn University

Academic year 2009


Thesis Title Spin Glass Phase in Random-Bond Ising Model  
By Mr. Luecha Tungchanachaiyanun  
Field of Study Physics  
Thesis Advisor Chatchai Srinitiwara Wong, Ph.D.


---

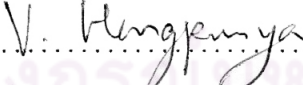
Accepted by the Faculty of Science, Chulalongkorn University in Partial Fulfillment of the Requirements for the Master's Degree


  
..... Dean of the Faculty of Science  
(Professor Supot Hannongbua, Ph.D.)

THESIS COMMITTEE

  
..... Chairman  
(Assistant Professor Patcha Chatraphorn, Ph.D.)

  
..... Thesis Advisor  
(Chatchai Srinitiwara Wong, Ph.D.)

  
..... Thesis Examiner  
(Varagorn Hengpunya, Ph.D.)

  
..... External Examiner  
(Supitch Khemmani, Ph.D.)

ลือชา ตั้งชนะชัยอนันต์: ภาวะแก้วสปินในแบบจำลองไอซิงที่มีพันธะแบบสุ่ม.

(SPIN GLASS PHASE IN RANDOM BOND ISING MODEL) อ. ที่ปรึกษา : อ. ดร.  
ฉัตรชัย ศรีนิติวรวงศ์, 69 หน้า.

แผนภาพเฟสของแบบจำลองไอซิงที่มีพันธะแบบสุ่มในโครงผลึกสองมิติแบบจัตุรัส ได้ศึกษา แบบจำลองที่ศึกษาใช้พื้นฐานจากแบบจำลองไอซิงที่มีพันธะแบบสุ่มที่การกระจายตัวของอันตรกิริยาแม่เหล็กเป็นแบบเกาส์เซียนแทนการกระจายตัวแบบเอกรูป จุดศูนย์กลางของการกระจายตัวเป็นบวกค่านั้นอันตรกิริยาส่วนใหญ่เป็นแม่เหล็กเฟอร์โร อย่างไรก็ตามความกว้างของการกระจายตัวสามารถเปลี่ยนได้ การเพิ่มขึ้นของความกว้างทำให้เกิดความไม่เป็นระเบียบของทิศทางของสปินในระบบ คาดการณ์ว่าเมื่อหางของการกระจายตัวไปถึงบริเวณอันตรกิริยาที่เป็นลบ ระบบที่อุณหภูมิต่ำจะปรากฏรอยต่อระหว่างเฟสแม่เหล็กเฟอร์โรและเฟสแก้วสปิน โดยการใช้ค่าความเป็นแม่เหล็กและค่าความเป็นแม่เหล็กแก้วสปิน เฟสทั้ง 3 ได้ปรากฏขึ้นในแผนภาพเฟส: 1 เฟสแม่เหล็กเฟอร์โร; 2 เฟสแก้วสปิน; 3 เฟสแม่เหล็กพารา ที่อุณหภูมิสูงระบบอยู่ในเฟสแม่เหล็กพารา ส่วนที่อุณหภูมิต่ำและการกระจายตัวของอันตรกิริยาแคบระบบอยู่ในเฟสแม่เหล็กเฟอร์โร รอยต่อระหว่างเฟสแม่เหล็กเฟอร์โรและเฟสแก้วสปินจะสังเกตได้เมื่อความกว้างของการกระจายตัวเพิ่มขึ้นที่อุณหภูมิต่ำ ส่วนอุณหภูมิวิกฤตสามารถหาได้โดยการใช้บิเนตอร์คูมูเลนต์ของความเป็นแม่เหล็กแก้วสปิน

ศูนย์วิทยทรัพยากร  
จุฬาลงกรณ์มหาวิทยาลัย

ภาควิชา ฟิสิกส์ ..... ลายมือชื่อนิสิต..... ลือชา ตั้งชนะชัยอนันต์  
สาขาวิชา ฟิสิกส์ ..... ลายมือชื่อ อ.ที่ปรึกษา..... อ.ดร. ฉัตรชัย ศรีนิติวรวงศ์  
ปีการศึกษา 2552

## 4972593623 :MAJOR PHYSICS

KEY WORDS: RANDOM-BOND ISING MODEL/SPIN GLASS PHASE/RSG  
TRANSITION

LUECHA TUNGCHANACHAIANUN : SPIN GLASS PHASE IN  
RANDOM-BOND ISING MODEL. THESIS ADVISOR : CHATCHAI  
SRINITIWARAWONG, PH.D., 69 pp.

The phase diagram of modified random-bond Ising model in two dimension square lattice has been investigated. The model is based on random-bond Ising model in which the distribution of magnetic interaction is Gaussian rather than the uniform distribution. The center of the distribution is positive so that most of the interactions are ferromagnetic. However the width of the distribution can be varied. The increasing of the width ( $J$ ) induces disorder to this system. It is expected that when the tail of the distribution reaches the negative interaction region, the system at low temperature shows the cross over between ferromagnetic phase and spin glass phase. By using magnetization and spin glass magnetization, three ordered phases appear in the  $J - T$  phase diagram: (1) ferromagnetic phase; (2) spin glass phase; (3) paramagnetic phase. At very high temperature the system is in paramagnetic phase. At low temperature and small width of the distribution, the system is in ferromagnetic phase. The cross over between ferromagnetic phase and spin glass phase is visible as the width of the interaction distribution is increased at low temperature. The critical temperatures have been obtained by using Binder cumulant of spin glass magnetization.

Department Physics ..... Student's signature *Luecha T.*.....

Field of study Physics ..... Advisor's signature *Chatchai Srinitiwara Wong*.....

Academic year 2009.....

# ACKNOWLEDGEMENTS

First I would like to express my wholehearted love to my father and mother for their love and support. I would also like to thank my advisor Dr. Chatchai Srinitiwara Wong for introducing me to this subject and for being very helpful during all states of my work in this thesis. Besides, I wish to mention my sincere thankfulness to Assist. Prof. Patcha Chatraphorn, Dr. Varagorn Hengpunya and Dr. Supitch Khemmani for many good suggestions in this thesis. In addition, I would like to thank all academics staff at the Physics Department for their helps. During this work on I have learned a lot of physics and many other skills such as programming and solving the large project. Finally, I would like to thank all my friends who associate and share a common fate with me.



ศูนย์วิทยทรัพยากร  
จุฬาลงกรณ์มหาวิทยาลัย

# CONTENTS

	page
Abstract (Thai) .....	iv
Abstract (English).....	v
Acknowledgements .....	vi
Contents .....	vii
List of Figures.....	xi
<b>1 INTRODUCTION.....</b>	<b>1</b>
<b>2 STATISTICAL MECHANICS.....</b>	<b>3</b>
2.1 Canonical ensemble . . . . .	3
2.2 Phase transition . . . . .	6
<b>3 THE MODELS.....</b>	<b>7</b>
3.1 The Ising model . . . . .	7
3.1.1 The Onsager solution . . . . .	8
3.2 Spin glass . . . . .	12
3.3 Random-bond Ising model (RBIM) . . . . .	17
3.4 Reentrant spin glass transition . . . . .	18
3.5 The modified Random-Bond Ising model . . . . .	19
3.6 Important parameters . . . . .	20
3.6.1 Heat capacity( $C_V$ ) . . . . .	21
3.6.2 Average magnetization( $m$ ) . . . . .	21

3.6.3	Magnetic susceptibility( $\chi$ ) . . . . .	22
3.6.4	Mean-square disorder average local moment( $q$ ) . . . . .	23
3.6.5	Binder cumulants( $U, g$ ) . . . . .	23
<b>4</b>	<b>SIMULATION PROCESS . . . . .</b>	<b>25</b>
4.1	State transition and Metropolis algorithm . . . . .	25
4.2	Simulation process . . . . .	26
4.3	Important parameters . . . . .	27
4.3.1	Energy( $E$ ) . . . . .	27
4.3.2	Heat capacity( $C_V$ ) . . . . .	28
4.3.3	Average magnetization( $m$ ) . . . . .	28
4.3.4	Magnetic susceptibility( $\chi$ ) . . . . .	28
4.3.5	Mean-square disorder average local moment( $q$ ) . . . . .	29
4.3.6	Binder cumulant( $U, g$ ) . . . . .	29
<b>5</b>	<b>RESULTS AND DISCUSSIONS . . . . .</b>	<b>31</b>
5.1	Simulation results . . . . .	31
5.1.1	Energy( $E$ ) . . . . .	31
5.1.2	Heat capacity( $C_V$ ) . . . . .	33
5.1.3	Average magnetization( $m$ ) . . . . .	35
5.1.4	Magnetic susceptibility( $\chi$ ) . . . . .	37
5.1.5	Mean-square disorder average local moment( $q$ ) . . . . .	39
5.1.6	Binder cumulant( $U, g$ ) . . . . .	41
5.2	Phase diagram . . . . .	43
<b>6</b>	<b>CONCLUSIONS . . . . .</b>	<b>46</b>
	References . . . . .	48



<b>Appendices</b> .....	<b>52</b>
<b>Appendix A : Using MPI</b> .....	<b>52</b>
A.1 Basic MPI concept .....	52
A.1.1 Parallel computational models .....	52
A.1.2 Advantages of the Message-Passing model .....	54
A.2 Setup the MPI .....	56
A.2.1 The lamboot command .....	56
A.2.2 The lamnodes command .....	59
A.2.3 Compiling MPI programs .....	59
A.3 Running the MPI .....	60
A.3.1 The MPI command .....	60
A.3.2 The mpiexec command .....	61
A.3.3 The mpitask command .....	62
A.3.4 The mpiclean command .....	63
A.4 Shutting down the LAM universe .....	63
<b>Appendix B : Parallel tempering</b> .....	<b>64</b>
B.1 Feedback-optimized temperature .....	65
<b>Vitae</b> .....	<b>70</b>

# LIST OF FIGURES

3.1	Gaussian distribution interaction of spin glass. . . . .	14
3.2	Uniform distribution interaction of spin glass. . . . .	14
3.3	Uniform distribution interaction of random-bond Ising model. . . . .	18
3.4	Gaussian distribution interaction with high disorder. . . . .	20
3.5	Gaussian distribution interaction with low disorder. . . . .	20
5.1	Energy as a function of temperature, $T$ , and the width of the interaction distribution $J$ . . . . .	32
5.2	Contour plot of energy diagram as a function of temperature, $T$ , and the width of the interaction distribution $J$ . . . . .	32
5.3	3-D diagram of heat capacity $C_V$ as a function of temperature, $T$ , and the width of the interaction distribution $J$ . . . . .	34
5.4	Contour plot of heat capacity $C_V$ as a function of temperature, $T$ , and the width of the interaction distribution $J$ . . . . .	34
5.5	3-D diagram of average magnetization $m$ as a function of temperature, $T$ , and the width of the interaction distribution $J$ . . . . .	36
5.6	Contour plot of average magnetization $m$ as a function of temperature, $T$ , and the width of the interaction distribution $J$ . . . . .	36
5.7	3-D diagram of magnetic susceptibility $\chi$ as a function of temperature, $T$ , and the width of the interaction distribution $J$ . . . . .	38
5.8	Contour plot of magnetic susceptibility $\chi$ as a function of temperature, $T$ , and the width of the interaction distribution $J$ . . . . .	38
5.9	3-D diagram of Mean-square disorder average local moment ( $q$ ) as a function of temperature, $T$ , and the width of the interaction distribution $J$ . . . . .	40

5.10 Contour plot of Mean-square disorder average local moment ( $q$ ) as a function of temperature, $T$ , and the width of the interaction distribution $J$ . . . . .	40
5.11 Magnetization Binder cumulant at $J = 0.25$ , $J = 0.50$ , $J = 0.75$ at difference system size. . . . .	41
5.12 Spin glass Binder cumulant at $J = 0.50$ , $J = 1.00$ , $J = 1.50$ , $J = 2.00$ at difference system size. . . . .	42
5.13 Phase diagram of modified random-bond Ising model. . . . .	44



ศูนย์วิทยทรัพยากร  
จุฬาลงกรณ์มหาวิทยาลัย

# CHAPTER 1

## INTRODUCTION

At the beginning of twentieth century, statistical mechanics was developed to explain many phenomena that involved many particles such as gas systems. It is able to establish the relationship between the macroscopic properties and microscopic properties in the classical regime. In the mean time, quantum mechanics was also developed in order to explain the phenomena that cannot be explained with classical mechanics. Combining quantum mechanics with statistical mechanics, the phenomena such as black body radiation [1], magnetism and phase transition can be explained [2, 3]. The problem is that the systems in statistical mechanics are stochastic systems in which the randomness is involved in the development of the future states of the system. In classical mechanics, most of the systems are deterministic that is no randomness is involved in the development of future states of the system. So the deterministic system can be solved by using analytic method to predict the evolution with time. In the system with many particles, it will become stochastic because the degrees of freedom lead to the chaotic. In the stochastic system, the evolution of system can not be predicted precisely by analytic method since the system involves the randomness of some degrees of freedom. However the stochastic system can be simulated with the modern computer by using random number generator to generate the stochastic process. The important point is that the random number generator must be a true random number generator otherwise the numbers will repeat again and the process will not become stochastic process. The evolution of the system will be controlled by transition probability which can be calculated from statistical mechanics.

One of the model that is used to describe magnetic systems is the Ising

model which was named after the physicist Ernst Ising. In his 1925 Ph.D. thesis [2], Ising solved the model for the 1 dimensional lattice where the solution shows that there is no phase transition. In the 2 dimensional lattice, however the solution shows the phase transition between ferromagnetic phase and paramagnetic phase [3]. Another model for describing magnetic systems is the spin glass model [4] which exhibits the new phase which can not be occurred in 2 dimensional Ising model.

In this thesis, we will investigate the magnetic phases that can occur in the modified random-bond Ising model. This model has been proposed based on the assumption that adding another material will cause the system to be distorted. By using computer simulation, the phase diagram and important parameters can be obtained.

In Chapter 2, the main discussions are focus on the fundamental idea on statistical mechanics. In Chapter 3, the basic model in which the modified random-bond Ising model is based on will be discussed. Then in Chapter 4, the main discussion is the results from computer simulation and the phase diagram. The conclusion is on Chapter 5.

ศูนย์วิทยทรัพยากร  
จุฬาลงกรณ์มหาวิทยาลัย

# CHAPTER 2

## STATISTICAL MECHANICS

This chapter is devoted exclusively to the basic idea of statistical mechanics. The discussion is mainly to show how the algorithm has been designed and implemented.

### 2.1 Canonical ensemble

Canonical ensemble is appropriate for describe systems not in an isolation, but in thermal equilibrium with a reservoir. The basic postulate in canonical ensemble is start with the system that is in contact with a larger system. The large system has constant temperature. Consider an isolated composite system made up of two subsystems whose Hamiltonians are  $H_1(p_1, x_1)$  and  $H_2(p_2, x_2)$  the number of particles in subsystems is written as  $N_1$  and  $N_2$ , respectively. Both  $N_1$  and  $N_2$  are macroscopically large and satisfies the condition  $N_2 \gg N_1$ . Consider a microcanonical ensemble of the composite system with total energy between  $E$  and  $E + \Delta E$ , the energy  $E_1$  and  $E_2$  of the subsystems can have any values satisfying

$$E < (E_1 + E_2) < E + \Delta E.$$

Although this includes a wide range of values for  $E_1$  and  $E_2$ , only one set of values, namely  $\bar{E}_1, \bar{E}_2$  is important. Assume that  $\bar{E}_2 \gg \bar{E}_1$ , let  $\Gamma_2(E_2)$  be the volume occupied by system 2 in its own  $\Gamma$  space. The probability of finding system 1 in a state within  $dp_1 dx_1$  of  $(p_1, x_1)$ , regardless of the state of system 2, is proportional to  $\Gamma_2(E_2) dp_1 dx_1$ , where  $E_2 = E - E_1$ . Therefore up to a proportionality constant

the density in  $\Gamma$  space for system 1 is

$$\rho(p_1, x_1) \propto \Gamma_2(E - E_1).$$

Since only the values near  $E_1 = \bar{E}_1$  are expected to be important, and  $\bar{E}_1 \ll E$ , the expansion can be performed as

$$\begin{aligned} K \log \Gamma_2(E - E_1) &= S_2(E - E_1) = S_2(E) - E_1 \left[ \frac{\partial S_2(E_2)}{\partial E_2} \right]_{E_2=E} + \dots \\ &\approx S_2(E) - \frac{E_1}{T}, \end{aligned}$$

where  $T$  is the temperature and  $S$  is an entropy, hence

$$\Gamma_2(E - E_1) \approx \exp \left[ \frac{1}{k} S_2(E) \right] \exp \left( - \frac{E_1}{kT} \right). \quad (2.1)$$

The first factor is independent of  $E_1$  and is thus a constant as far as the small subsystem is concerned. Since  $E_1 = H_1(p_1, x_1)$ , the ensemble density for the small subsystem can be written as

$$\rho(p, x) = e^{-H(p,x)/kT} \quad (2.2)$$

where the subscript 1 labeling the subsystem has been omitted. Since the temperature of the larger subsystem is at constant  $T$ , it behaves like heat reservoir and it keeps the total temperature of the system at constant. The ensemble defined by (2.2), appropriate for a system whose temperature is determined through a contact with a heat reservoir, is called the canonical ensemble.

The partition function of the system can be calculated by integrating over the volume in  $\Gamma$  space occupied by the canonical ensemble:

$$Z_N(V, T) \equiv \int e^{-\beta H(p,x)} \frac{d^{3N}p d^{3N}x}{N! h^{3N}} \quad (2.3)$$

where  $\beta = 1/kT$ , and the constant  $h$  has the dimension of *momentum*  $\times$  *distance* to make  $Z_N$  dimensionless. The factor  $1/N!$  appears, in accordance with the rule of correct Boltzmann counting. These constants are of no importance for the equation of the state.

The canonical ensemble is mathematically equivalent to the microcanonical ensemble in the sense that although the canonical ensemble contains system of all energies, the overwhelming majority of them have the same energy. To do this,

the mean square fluctuation of energy must be calculated in canonical ensemble.

The average energy is

$$U = \langle H \rangle = \frac{\int H e^{-\beta H} dp dx}{\int e^{-\beta H} dp dx}. \quad (2.4)$$

Hence

$$\begin{aligned} \int [U - H(p, x)] e^{\beta(A(V, T) - H(p, x))} dp dx &= 0, \\ \frac{\partial U}{\partial \beta} + \int e^{\beta(A - H)} (A - H) \left( A - H - T \frac{\partial A}{\partial T} \right) &= 0, \end{aligned} \quad (2.5)$$

where  $A(V, T)$  is the Helmholtz free energy. This can be rewritten in the form

$$\frac{\partial U}{\partial \beta} + \langle (U - H)^2 \rangle = 0. \quad (2.6)$$

Therefore the mean square fluctuation of the energy is

$$\langle H^2 \rangle - \langle H \rangle^2 = \langle (U - H)^2 \rangle = -\frac{\partial U}{\partial \beta} = kT^2 \frac{\partial U}{\partial T}$$

or

$$\langle H^2 \rangle - \langle H \rangle^2 = kT^2 C_V, \quad (2.7)$$

for a macroscopic system  $\langle H \rangle \propto N$  and  $C_V \propto N$ , hence (2.7) is normal fluctuation. As  $N \rightarrow \infty$ , almost all systems in the ensemble have the energy  $\langle H \rangle$ , which is the internal energy. Therefore the canonical ensemble is equivalent to the microcanonical ensemble in thermodynamic limit.

In the canonical ensemble, the systems are distributed in  $\Gamma$  space according to the density function  $\rho(p, x) = \exp[-\beta H(p, x)]$ . The distribution in energy is obtained by counting the number of points on energy surfaces. The peak in the distribution of the system energy occurs with this reason. The sharpness of the peak is due to the rapidly increasing of the area of the energy surface as  $E$  increase. For an  $N$ -body system this area increases like  $e^E$ , where  $E \propto N$ .

From a physical point of view, a microcanonical ensemble must be equivalent to a canonical ensemble. A microcanonical substance has the extensive property. Any part of the substance must be in equilibrium with the rest of the substance, which serves as a heat reservoir that defines a temperature for the part which has been focused. Therefore the whole substance must have a well-defined temperature.



## 2.2 Phase transition

A phase transition is signaled by a singularity in a thermodynamic potential such as the free energy. If there is a finite discontinuity in one or more of the first derivatives of the appropriate thermodynamic potential, the transition is termed first-order. For a magnetic system the Helmholtz free energy  $A(V, T)$  is the appropriate potential with a discontinuity in the magnetization showing that the transition is first-order. If the first derivatives are continuous but second derivatives are discontinuous, the transition will be described as higher order, continuous or critical. This type of transition corresponds to a divergent of susceptibility, an infinite correlation length and a power law decay of correlation.



# CHAPTER 3

## THE MODELS

This chapter is devoted exclusively to the basic idea of Ising model, random-bond Ising model, spin glass model and modified random-bond Ising model. Mainly, the discussion is about how the model has been formulated from physical systems and the properties of each model will be explored. Before we start with the random-bond and spin glass model, the basic idea of Ising model in which both models are based on must be reviewed first.

### 3.1 The Ising model

The Ising model, is named after the physicist Ernst Ising after he solved the model for the 1 dimension magnetic system in his 1925 Ph.D. thesis [2]. The Ising model is defined on a discrete collection of spins. In the Ising model, the system consists of an array of  $N$  fixed points called lattice that form an  $n$ -dimensional periodic lattice. The geometrical structure of the lattice may be cubic or hexagonal. Associated with each lattice site is a spin variable  $S_i$  which is a number that is either  $+1$  or  $-1$ . If  $S_i = +1$ , the  $i$ th site is said to have a spin up, and if  $S_i = -1$ , it is said to have a spin down. A given set of number  $\{S_i\}$  specifies a configuration of the system. The Hamiltonian of the system in the configuration specified by  $\{S_i\}$  is defined as

$$H = - \sum_{\langle ij \rangle} JS_i S_j, \quad (3.1)$$

where the symbol  $\langle ij \rangle$  denotes a nearest-neighbor pair of spins. There is no distinction between  $\langle ij \rangle$  and  $\langle ji \rangle$ . Thus the sum over  $\langle ij \rangle$  contains  $\gamma N/2$  terms, where  $\gamma$  is the number of nearest neighbors of any given site. The magnetic interaction

$J$  is constant. Magnetic interaction tries to align all spins on the lattice in the optimal direction hence the ordered phase, while thermal energy tries to break the order. For each pair, if the interaction is positive, the spins try to align in the same direction. If the interaction is negative, the spins try to align in the opposite direction. In one dimension, the solution admits no phase transition. The Ising model undergoes a phase transition between an ordered and disordered phase in 2 dimensions or more.

### 3.1.1 The Onsager solution

The partition function of the Ising model in two dimensions on a square lattice can be mapped into a 2 dimensional of free fermions ( $S = \pm 1$ ) [3]. Consider a square lattice of  $N = n^2$ , the lattice consists of  $n$  rows and  $n$  columns of spins. Let the lattice be enlarged by one row and one column with the requirement that the configuration of the  $(n + 1)$  row and  $(n + 1)$  column will be identical to that of the first row and the first column respectively. This boundary condition endows the lattice with the topology of a torus. Let  $\mu_\alpha$  ( $\alpha = 1, \dots, n$ ) denotes the collection of all the spin coordinates of the  $\alpha$  row:

$$\mu_\alpha \equiv \{S_1, S_2, \dots, S_n\}_\alpha. \quad (3.2)$$

A configuration of the entire lattice is then specified by  $\{\mu_1, \dots, \mu_n\}$ . By assumption, the  $\alpha$  row interacts only the  $(\alpha - 1)$  and the  $(\alpha + 1)$  row. Let  $E(\mu_\alpha, \mu_{\alpha+1})$  be the interaction energy between the  $\alpha$  and  $\alpha + 1$  row:

$$E(\mu, \mu') = -J \sum_{k=1}^n S_k S'_k. \quad (3.3)$$

Let  $E(\mu_\alpha)$  be the interaction energy of the spins within the  $\alpha$  row:

$$E(\mu) = -J \sum_{k=1}^n S_k S_{k+1}. \quad (3.4)$$

The  $\mu$  and  $\mu'$  respectively denote the collection of spin coordinates in two neighboring rows. The total energy of the lattice for the configuration  $\{\mu_1, \dots, \mu_n\}$  is given by

$$E\{\mu_1, \dots, \mu_n\} = \sum_{\alpha=1}^n [E(\mu_\alpha, \mu_{\alpha+1}) + E(\mu_\alpha)].$$

The partition function is

$$Z(T) = \sum_{\mu_1} \cdots \sum_{\mu_n} \exp\left\{-\beta \sum_{\alpha=1}^n [E(\mu_\alpha, \mu_{\alpha+1}) + E(\mu_\alpha)]\right\}. \quad (3.5)$$

Let the matrix element of  $2^n \times 2^n$  matrix  $P$  be defined as

$$\langle \mu | P | \mu' \rangle \equiv e^{-\beta [E(\mu, \mu') + E(\mu)]}. \quad (3.6)$$

Then

$$\begin{aligned} Z(T) &= \sum_{\mu_1} \cdots \sum_{\mu_n} \langle \mu_1 | P | \mu_2 \rangle \langle \mu_2 | P | \mu_3 \rangle \cdots \langle \mu_n | P | \mu_1 \rangle \\ &= \sum_{\mu_1} \langle \mu_1 | P^n | \mu_1 \rangle = \text{Tr} P^n. \end{aligned} \quad (3.7)$$

The matrix elements of  $P$  can be obtained in another form

$$\langle S_1, \dots, S_n | P | S_1, \dots, S'_m \rangle = \prod_{k=1}^n e^{\beta J S_k S_{k+1}} e^{\beta J S_k S'_k}. \quad (3.8)$$

Define two  $2^n \times 2^n$  matrices  $V'_1$  and  $V_2$  whose matrix elements are respectively given by

$$\langle S_1, \dots, S_n | V'_1 | S_1, \dots, S'_m \rangle \equiv \prod_{k=1}^n e^{\beta J S_k S'_k}, \quad (3.9)$$

$$\langle S_1, \dots, S_n | V_2 | S_1, \dots, S'_m \rangle \equiv \delta_{S_1 S'_1} \cdots \delta_{S_n S'_n} \prod_{k=1}^n e^{\beta J S_k S_{k+1}}. \quad (3.10)$$

It can be verified that

$$P = V_2 V'_1. \quad (3.11)$$

The  $V'_1$  is the product of  $n$   $2 \times 2$  identical matrices

$$V'_1 = a \times a \times \cdots \times a \quad (3.12)$$

where

$$\langle S | a | S' \rangle = e^{\beta J S S'}.$$

Therefore

$$a = \begin{bmatrix} e^{\beta J} & e^{-\beta J} \\ e^{-\beta J} & e^{\beta J} \end{bmatrix} = e^{\beta J} + e^{-\beta J} X \quad (3.13)$$

where  $X$  is the  $2 \times 2$  Pauli spin matrices :

$$X \equiv \begin{bmatrix} 0 & 1 \\ 1 & 0 \end{bmatrix}, Y \equiv \begin{bmatrix} 0 & -i \\ i & 0 \end{bmatrix}, Z \equiv \begin{bmatrix} 1 & 0 \\ 0 & -1 \end{bmatrix}. \quad (3.14)$$

By using the mathematic identity, the matrix  $a$  can be rewritten as

$$a = \sqrt{2 \sinh(2\beta J)} e^{\theta X} \quad (3.15)$$

where

$$\tanh \theta \equiv e^{-2\beta J}.$$

Hence

$$\begin{aligned} V_1' &= [2 \sinh(2\beta J)]^{n/2} e^{\theta X} \times e^{\theta X} \times \dots \times e^{\theta X}. \\ &= [2 \sinh(2\beta J)]^{n/2} V_1 \end{aligned} \quad (3.16)$$

where

$$\begin{aligned} V_1 &= \prod_{\alpha=1}^n e^{\theta X}, \\ \tanh \theta &\equiv e^{-2\beta J}. \end{aligned}$$

A calculation of matrix elements shows that

$$V_2 = \prod_{\alpha=1}^n e^{\beta J Z_{\alpha} Z_{\alpha-1}}. \quad (3.17)$$

Therefore

$$P = [2 \sinh(2\beta J)]^{n/2} V_2 V_1. \quad (3.18)$$

This lead to the following:

$$\lim_{N \rightarrow \infty} \frac{1}{N} \log Z(T) = \frac{1}{2} \log [2 \sinh(2\beta J)] + \lim_{n \rightarrow \infty} \frac{1}{n} \log \Lambda \quad (3.19)$$

where  $\Lambda$  is the largest value of  $V$  and

$$V = V_1 V_2. \quad (3.20)$$

This formula are valid if all eigenvalues of  $V$  are positive and if  $\lim_{n \rightarrow \infty} n^{-1} \log \Lambda$  exist. The largest value of  $V$  can be calculated as

$$\Lambda = e^{1/2(\gamma_1 + \gamma_3 + \gamma_5 + \dots + \gamma_{2n-1})} \quad (3.21)$$

where

$$\begin{aligned} \cosh \gamma_k &= z \cosh 2\phi \cosh 2\theta - \cos \frac{\pi k}{n} \sinh 2\pi \sinh 2\theta \\ k &= 0, 1, \dots, 2n-1 \end{aligned}$$

and

$$\phi = \beta J.$$

The Helmholtz free energy per spin can be obtained as

$$a(T) = -\frac{1}{\beta} \log(2 \cosh 2\beta J) - \frac{1}{2\pi\beta} \int_0^\pi \log \frac{1}{2} \left( 1 + \sqrt{1 - \left( \frac{2}{\cosh 2\phi \coth 2\phi} \right)^2 \sin^2 \phi} \right) d\phi \quad (3.22)$$

and the internal energy per spin can be obtained as

$$\begin{aligned} u(T) &= \frac{d}{d\beta} [\beta a(T)] \\ &= -J \coth 2\beta J \left[ 1 + \frac{2}{\pi} \kappa' K_1(\kappa) \right] \end{aligned} \quad (3.23)$$

where  $K_1(\kappa)$  is a tabulated function, the complete elliptic integral of the first kind:

$$K_1(\kappa) \equiv \int_0^{\pi/2} \frac{d\phi}{\sqrt{1 - \kappa^2 \sin^2 \phi}} \quad (3.24)$$

and

$$\begin{aligned} \kappa &\equiv \frac{2 \sinh 2\beta J}{\cosh^2 2\beta J} \\ \kappa' &\equiv 2 \tanh^2 2\beta J - 2 \\ \kappa^2 + \kappa'^2 &= 1. \end{aligned}$$

The specific heat  $c(T)$  is shown to be

$$c(T) = \frac{2k}{\pi} (\beta J \coth 2\beta J)^2 \{ 2K_1(\kappa) - 2E_1(\kappa) - 1(1 - \kappa') \left[ \frac{\pi}{2} + \kappa' K_1(\kappa) \right] \} \quad (3.25)$$

where  $E_1(\kappa)$  is a tabulated function, the complete elliptic integral of the second kind:

$$E_1(\kappa) \equiv \int_0^{\pi/2} \sqrt{1 - \kappa^2 \sin^2 \phi} d\phi. \quad (3.26)$$

The elliptic integral  $K_1(\kappa)$  has a singularity at  $\kappa = 1$  (or  $\kappa' = 0$ ),

$$K_1(\kappa) \approx \log \frac{4}{\kappa'}, \quad \frac{dK_1(\kappa)}{d\kappa} \approx \frac{\pi}{2} \quad (3.27)$$

$$E_1(\kappa) \approx 1. \quad (3.28)$$

Thus all thermodynamic functions have a singularity of some kind at  $T = T_c$ , where  $T_c$  is such that

$$\begin{aligned} 2 \tanh^2 \frac{2J}{kT_c} &= 1 \\ kT_c &= (2.269185)J. \end{aligned} \quad (3.29)$$

Other relations satisfied by  $T_c$  are

$$\begin{aligned} e^{-J/kT_c} &= \sqrt{2} - 1, \\ \cosh \frac{2J}{kT_c} &= \sqrt{2}, \\ \sinh \frac{2J}{kT_c} &= 1. \end{aligned}$$

Thus near  $T = T_c$

$$c(T) \approx \frac{2k}{\pi} \left( \frac{2J}{kT_c} \right)^2 \left[ -\log \left| 1 - \frac{T}{T_c} \right| + \log \left( \frac{kT_c}{2J} \right) - \left( 1 + \frac{\pi}{4} \right) \right]. \quad (3.30)$$

It approaches infinity logarithmically as  $|T - T_c| \rightarrow 0$ . The internal energy is continuous at  $T = T_c$ . Thus the phase transition at  $T = T_c$  involves no latent heat.

To justify calling the phenomenon at  $T = T_c$  a phase transition, the long range-order i.e., the spontaneous magnetization must be examined. To calculate the spontaneous magnetization, the derivative of the free energy with respect to  $H$  at  $H = 0$  has to be calculated. The result shows that the spontaneous magnetization per spin is

$$m(T) = \begin{cases} 0 & (T > T_c) \\ \{1 - [\sinh(2\beta J)]^{-4}\}^{\frac{1}{8}} & (T < T_c). \end{cases} \quad (3.31)$$

## 3.2 Spin glass

The spin glasses model was proposed by S. F. Edwards and P. W. Anderson in 1975 [4]. The expression spin glass was originally coined to describe some magnetic alloys in which there was observed non-periodic freezing of the orientation of the magnetic moment or spin, coupled with slow response and linear low temperature heat capacity characteristic of conventional glasses [5, 6]. The attempt to understand the cooperative physics of such alloys has exposed many previously unknown and unanticipated fundamental concepts and led to the devising of new analytical, experimental and computer simulation techniques. Spin glass model has been one of the interesting problems of complex systems. Such problems are ubiquitous, not only through out the breadth of condensed matter physics but

also biology, evolution, organizational dynamics, hard-optimization, and environmental and social structures. In consequence the expression spin glass has now taken on a wider interpretation to refer to complex glassy behavior arising from a combination of quenched disorder and competitive interactions or constraints, and to systems exhibiting such behavior. Spin glass behavior requires two essential ingredients. These are quenched disorder and frustration.

Quenched disorder refers to constrained disorder in the interactions between the spins and/or their locations. The spin orientations themselves are variables, governed by the interactions, external fields and thermal fluctuations. These spins are free to order or not as their dynamics or thermodynamics tell them. The spin glass phase is an example of spontaneous operatic freezing or order of the spin orientations in the presence of the constrained disorder of the interactions or spin locations.

Frustration refers to the conflicts between interactions, or other spin-ordering forces, such that not all can be obeyed simultaneously.

These features are readily visualized in a simple model of Hamiltonian appropriate to an idealization of magnetic interactions between atoms with defined local moment

$$H = - \sum_{\langle ij \rangle} J_{ij} S_i S_j, \quad (3.32)$$

where the  $J_{ij}$  measures the magnetic exchange interaction between the pair of spins  $(ij)$ . The variables are the  $\{S_i\}$ , while the  $\{J_{ij}\}$  are quenched/constrained. Pairs of spins get different ordering instructions through the various paths which link  $i$  and  $j$ , either directly or via intermediate spins and then gives rise to the frustration. The form of interactions distribution  $P(J_{ij})$  can be Gaussian, uniform or bimodal distribution such as the Figures 3.1 and 3.2 while the average of the interactions distribution equal to zero.

The most studied models of spin glass are

- The Edwards Anderson (EA) model [4]: The spins belong to a finite dimensional lattice of dimension  $D$ : Only nearest neighbor interactions are different from zero and their variance is  $D^{-1/2}$ .
- The Bethe lattice model [7, 8, 9]: The spins are on a random lattice and



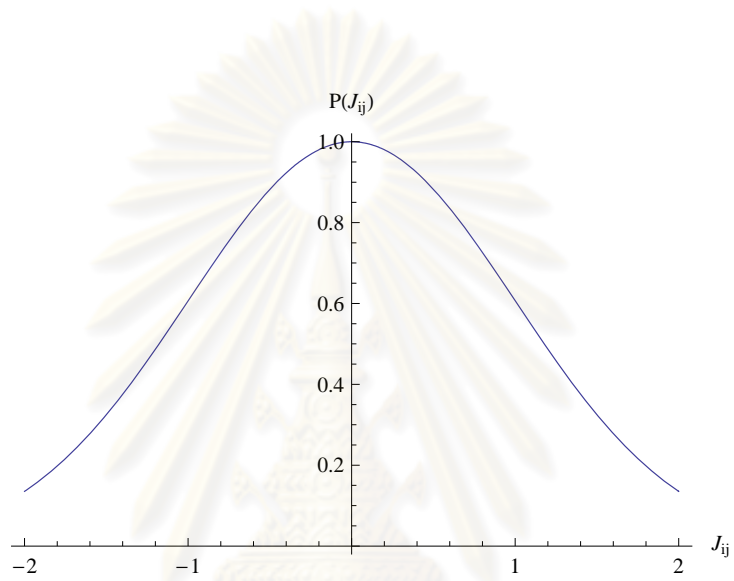


Figure 3.1: Gaussian distribution interaction of spin glass.

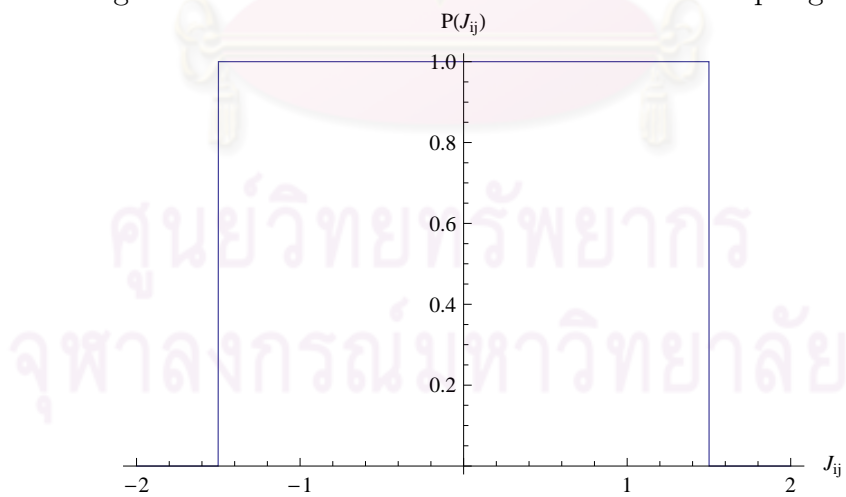


Figure 3.2: Uniform distribution interaction of spin glass.

only  $Nz/2$   $J$ 's are different from zero: They have variance  $z^{-1/2}$ . The coordination number is  $z$ .

- The Sherrington-Kirkpatrick (SK) model [10]: All  $J$ 's are random and different from zero, with a Gaussian or a bimodal distribution with variance  $N^{-1/2}$ . The coordination number is  $N - 1$  and it goes to infinity with  $N$  [11, 12].

The SK model is the special case of the EA model when the dimension goes to infinity. As far as the free energy is concerned, the following rigorous results can be obtained:

$$\begin{aligned}\lim_{z \rightarrow \infty} \text{Bethe}(z) &= SK, \\ \lim_{D \rightarrow \infty} \text{Edwards Anderson}(D) &= SK, \\ \lim_{R \rightarrow \infty} \text{finite range EA}(R) &= SK.\end{aligned}$$

A natural corollary of this recognition of the key ingredients is experimentally the behavior should not be restricted to metallic systems, provided one has disorder and frustration, and indeed the effects have now been seen in several insulating alloys. The canonical insulating example is  $Eu_xSr_{1-x}S$  in which only  $Eu$  is magnetic material and for which the nearest-neighbor interactions are ferromagnetic, next-nearest interactions are antiferromagnetic. Another example is  $Rb_2Cu_xCo_{1-x}F_4$  which exhibits the spin glass properties.

Consider the SK model that  $N$  Ising spins interact through an infinite-ranged exchange interactions which are independently distributed with a Gaussian probability density [10], the  $J_{ij}$  distributed according to

$$p(J_{ij}) = \frac{1}{(2\pi)^{1/2}J} \exp[-(J_{ij} - J_0)^2/2J^2], \quad (3.33)$$

where  $J_0$  and  $J$  scaled by

$$J_0 = \tilde{J}_0/N, J = \tilde{J}/N^{1/2}. \quad (3.34)$$

The averaged Helmholtz free energy may be expressed as

$$\begin{aligned}A &= -kT \lim_{n \rightarrow 0} n^{-1} \left\{ \int \prod_{(ij)} [p(J_{ij}) dJ_{ij}] Tr_n \exp\left( \sum_{\alpha=1, \dots, n} \sum_{i \neq j} J_{ij} S_i^\alpha S_j^\alpha / 2kT \right) - 1 \right\} \\ &= -kT \lim_{n \rightarrow 0} n^{-1} \left\{ Tr_n \exp\left( \sum_{i \neq j} \left[ \sum_{\alpha} S_i^\alpha S_j^\alpha J_0 / 2kT + \sum_{\alpha, \beta} S_i^\alpha S_j^\alpha S_i^\beta S_j^\beta J^2 / 4(kT)^2 \right] \right) - 1 \right\},\end{aligned}$$

where  $\alpha$  and  $\beta$  label  $n$  dummy replicas. Reordering and dropping terms which vanish in the thermodynamics limit yields

$$A = -kT \lim_{n \rightarrow 0} n^{-1} \{ \exp[J^2 N^2 n / 4(kT)^2] \times Tr_n \exp[\sum_{\alpha\beta} (\sum_i S_i^\alpha S_i^\beta)^2 J^2 / 2(kT)^2 + \sum_\alpha (\sum_i S_i^\alpha)^2 J_0 / 2kT] - 1 \} \quad (3.35)$$

where  $(\alpha\beta)$  refers to combinations of  $\alpha$  and  $\beta$  with  $\alpha \neq \beta$ . The Helmholtz free energy can be calculated as

$$A = NkT \{ -\tilde{J}^2(1-q)^2 / (2kT)^2 + \tilde{J}_0 m^2 / 2kT - (2\pi)^{-1/2} \int \exp(-z^2/2) \ln[2 \cosh(\tilde{J}q^{1/2}z/kT + \tilde{J}_0 m/kT)] dz \}. \quad (3.36)$$

Parameters  $q$  and  $m$  satisfy the simultaneous equations

$$\bar{q} = 1 - (2\pi)^{-1/2} \int \exp(-z^2/2) \cosh^{-2}[\tilde{J}q^{1/2}/kT + \tilde{J}_0 m/kT] dz, \quad (3.37)$$

$$\bar{m} = (2\pi)^{-1/2} \int \exp(-z^2/2) \tanh[(\tilde{J}q^{1/2}/kT)z + \tilde{J}_0 m/kT] dz. \quad (3.38)$$

To show the physical significance of  $\bar{m}$  and  $\bar{q}$ , the thermal average of the spin at site  $i$ ,  $\langle S_i \rangle$ , and its square may be written as

$$\langle S_i \rangle = \frac{\partial}{\partial h} \ln Tr \exp(\sum_{i \neq j} S_i^\alpha S_j^\alpha / 2kT + h S_i^\alpha)_{h=0}, \quad (3.39)$$

$$\langle S_i \rangle^2 = \frac{\partial}{\partial h'} \ln Tr \exp(\sum_{i \neq j} J_{ij} (S_i^\alpha S_j^\alpha + S_i^\beta S_j^\beta) / 2kT + h' S_i^\alpha S_i^\beta)_{h'=0}. \quad (3.40)$$

Parameters  $\alpha \neq \beta$  are dummy labels. Average over the  $J_{ij}$  distribution, which denote by  $[\dots]$ , the  $[\langle S_i \rangle]$  and  $[\langle S_i \rangle^2]$  are given by taking the  $n \rightarrow 0$  limit respectively of  $\langle S_i^\alpha \rangle$  and  $\langle S_i^\alpha \times S_i^\beta \rangle_{\alpha \neq \beta}$  evaluated for the system characterized by the  $J$ -averaged  $n$ -ensemble partition function. This result is valid for finite-ranged interactions as well as infinite-ranged ones. Thus [13]

$$\bar{m} \equiv [\langle S_i \rangle], \quad (3.41)$$

$$\bar{q} \equiv [\langle S_i \rangle^2] \quad (3.42)$$

independent of  $i$ . The notable point is that a reentrant spin glass transition occurs at the phase boundary between the ferromagnetic phase and the spin glass phase. In Sherrington and Kirkpatrick's paper, these phases can be distinguished by

the average magnetization  $\overline{m}$  and mean-square disorder average local moment  $\overline{q}$ . Hence non-zero  $\overline{q}$  implies a cooperatively frozen magnetic state while non-zero  $\overline{m}$  implies that that frozen state has a ferromagnetic component. These phases can be categorized [10, 13] as

1. paramagnetic if both  $\overline{m}$  and  $\overline{q}$  are zero.
2. ferromagnetic if both  $\overline{m}$  and  $\overline{q}$  are non-zero.
3. spin glass if  $\overline{q}$  is non-zero but  $\overline{m}$  is zero.

The average magnetization  $m$  and mean-square disorder average local moment  $\overline{q}$  are defined by

$$\overline{m} = [\langle S_i \rangle], \overline{q} = [\langle S_i \rangle^2].$$

### 3.3 Random-bond Ising model (RBIM)

If a typical antiferromagnet like  $\text{FeCl}_2$  is mixed with an isostructural nonmagnetic material like  $\text{CoCl}_2$  or  $\text{NiCl}_2$ , diluted antiferromagnets can be obtained. Within a uniform external field, a large degree of frustration is induced and a completely new universality class emerges. The random-bond Ising model is defined as

$$H = - \sum_{\langle ij \rangle} J_{ij} S_i S_j \quad (3.43)$$

with  $J_{ij} \geq 0$  is ferromagnetic interactions strengths between neighboring spins. These are random quenched variables, which mean that they are distributed according to some probability distribution and fixes right from the beginning. In the RBIM, the interactions are in the form of probability distribution [14], e.g., Gaussian [15], uniform [14], bimodal [16], etc. The example of the interaction distribution is shown in Figure 3.3.

Since the interaction are all ferromagnetic, the ground state is simply given by  $S_i = +1$  for all sites  $S_i$  or  $S_i = -1$  for all sites  $S_i$ . This induces an interface

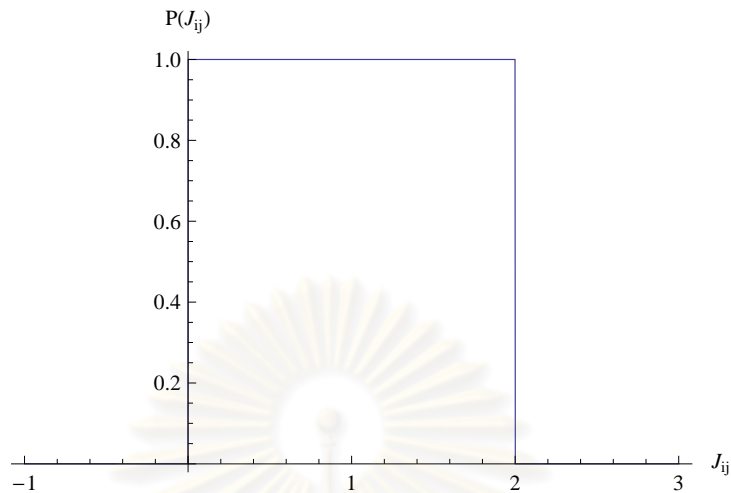


Figure 3.3: Uniform distribution interaction of random-bond Ising model.

through the sample where bonds have to be broken. If all bonds have the same strength  $J_{ij} = J$ , the system would become a pure Ising model. Because of the randomness of the  $J_{ij}$ , it is energetically more favorable to break weak bonds: the interface becomes distorted and its shape is rough. This model has also been used to describe fractures in materials where the  $J_{ij}$  represents the local force needed to break the material and it is assumed that the fracture occurs along the surface of minimum total rupture force.

### 3.4 Reentrant spin glass transition

A reentrant spin glass (RSG) transition occurs at the phase boundary between the ferromagnetic and the spin glass phase. That is, as the temperature is decreased from a high temperature, the magnetization that grows in the ferromagnetic phase vanishes at the phase boundary. The spin glass phase realized at lower temperatures is characterized by ferromagnetic cluster. It is believed that the phase diagram arises from the competition between ferromagnetic and antiferromagnetic interactions. Nevertheless, these phase diagrams have not yet been understood theoretically. Several models have been proposed for explaining the RSG transition. One of the earliest models to explain the reentrant spin glass transition is the Sherrington-Kirkpatrick spin glass model. The model exhibits the reentrant spin glass transition but does not fit well with the experimental data.

There are many experimental data showing that the reentrant spin glass transition exists in the phase diagram of some composite alloys [5], [17]. By varying the ratio of each ingredient and temperature, the material exhibits the ferromagnetic phase, paramagnetic phase and spin glass phase. When an Ising system is rapidly quenched from a high temperature to a temperature below  $T_c$ , it condenses into a non-equilibrium configuration built up of a great number of domains. In the subsequent evolution towards equilibrium, larger domains tend to grow at the expense of smaller ones. The driving force of this process is the lowering of the surface energy associated with the domain walls. In the system with randomly added impurities that do not destroy the ordered phase, the situation is substantially more complicated. The impurities, acting as pinning sites for domain walls, severely slow down the ordering dynamics.

### 3.5 The modified Random-Bond Ising model

The random-bond Ising model and Edwards-Anderson spin glass model both are based on 2 dimensional Ising model but using the difference set of interaction distribution. In the experiments [5],[17], there are phase transitions between ferromagnetic, paramagnetic and spin glass which is called reentrant spin glass transition. In spin glass model, the interactions are distributed in the form of Gaussian distribution, the interactions of random-bond Ising model are however difference. In order to explain this transition, the model has been modified with the hypothesis that adding another material will cause the system to become distorted. In our assumption the distortion corresponds to the width of the magnetic interaction. The width of the interaction become wider with the increasing of the distortion and the transition between different phases is expected. The Hamiltonian of the system can be written as

$$H = - \sum_{\langle ij \rangle} J_{ij} S_i S_j, \quad (3.44)$$

while the interactions  $J_{ij}$  are distributed according to

$$p(J_{ij}) = [(2\pi)^{1/2} J]^{-1} \exp[-(J_{ij} - J_0)^2 / 2J^2], \quad (3.45)$$

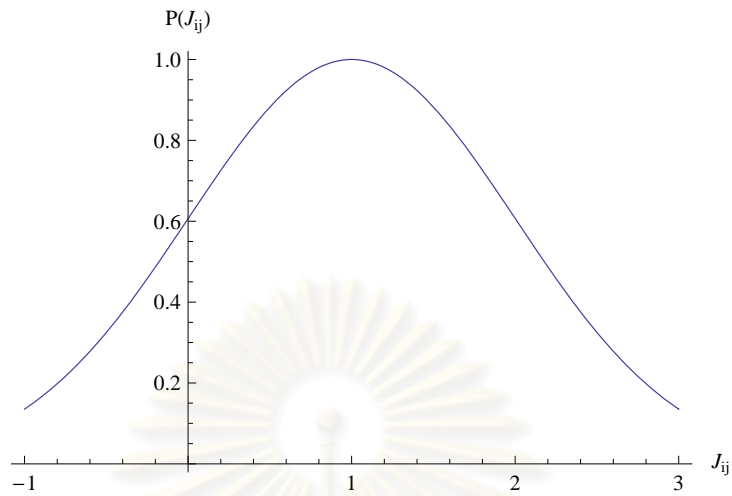


Figure 3.4: Gaussian distribution interaction with high disorder.

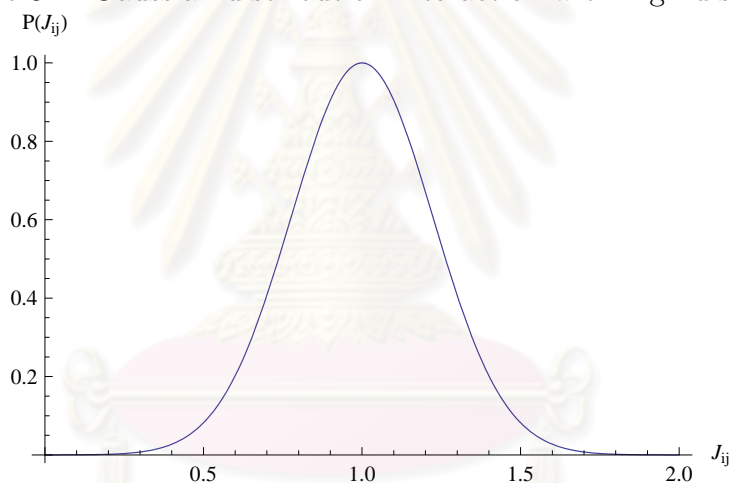


Figure 3.5: Gaussian distribution interaction with low disorder.

and the interactions are accounted only the nearest neighbor sites. Parameter  $J$  indicates the width of interactions' distribution as shown in the Figures 3.4 and 3.5. This value also indicates the degree of disorder of the system.  $J_0$  is the center of distribution which can be set to match with the experiments.

### 3.6 Important parameters

In statistical mechanics, there are many important parameters. Each parameter has different physical meaning.

### 3.6.1 Heat capacity( $C_V$ )

The heat capacity  $C_V$  represents the amount of energy required to increase the temperature of an object by a certain temperature interval. Heat capacity is an extensive property because its value is proportional to the amount of material in the system. The heat capacity can be defined as

$$C_V = \frac{\partial[\langle E \rangle]}{\partial T}. \quad (3.46)$$

The heat capacity is related to specific heat capacity  $c_v$  by

$$c_v = \frac{C_V}{V}. \quad (3.47)$$

The average energy of the system can be calculated from

$$\begin{aligned} \langle E \rangle &= \frac{\sum H e^{-H/kT}}{Z} \\ &= \frac{kT^2}{Z} \frac{\partial Z}{\partial T} \end{aligned} \quad (3.48)$$

and

$$\begin{aligned} \langle E^2 \rangle &= \frac{\sum H^2 e^{-H/kT}}{Z} \\ &= \frac{kT^4}{Z} \frac{\partial^2 Z}{\partial T^2}. \end{aligned} \quad (3.49)$$

By using the equation above, the heat capacity can be reformulated as

$$\begin{aligned} C_V &= kT^2 \frac{\partial}{\partial T} \left( \frac{1}{Z} \frac{\partial Z}{\partial T} \right) \\ &= \frac{kT^2}{Z} \frac{\partial^2 Z}{\partial T^2} - \frac{kT^2}{Z^2} \left( \frac{\partial Z}{\partial T} \right)^2 \\ &= \frac{[\langle E^2 \rangle] - [\langle E \rangle]^2}{T^2}. \end{aligned} \quad (3.50)$$

The equation states that the heat capacity can be measured from the fluctuations in the energy.

### 3.6.2 Average magnetization( $m$ )

The average magnetization indicates the magnetic phase of the system in the macroscopic scale. The average magnetization is

$$m = [\langle S_i \rangle]. \quad (3.51)$$



If most of the spins are align in the same direction, the average magnetization will not be zero. This means that the system has finite magnetization. In other hand, if the spins in the system align in up and down direction equally or randomly, the average magnetization will be zero. In this situation, system has no magnetization.

### 3.6.3 Magnetic susceptibility( $\chi$ )

The magnetic susceptibility  $\chi$  represents the degree of magnetization of a material in response to an applied magnetic field. It can be defined as

$$\chi = \frac{\partial[\langle m \rangle]}{\partial H}. \quad (3.52)$$

If the Hamiltonian  $H(\{S_i\}, H)$  depends on spin configuration  $\{S_i\}$  and magnetic field  $H$ , the partition function of the system can be written as

$$Z(H, T) = \sum e^{-\frac{H(\{S_i\}, H)}{kT}}. \quad (3.53)$$

The average magnetization of the system can be calculated from

$$\begin{aligned} \langle m \rangle &= \frac{\sum m e^{-\frac{H(\{S_i\}, H)}{kT}}}{Z(H, T)} \\ &= \frac{kT}{Z(H, T)} \frac{\partial Z(H, T)}{\partial H} \end{aligned} \quad (3.54)$$

and

$$\begin{aligned} \langle m^2 \rangle &= \frac{\sum m^2 e^{-\frac{H(\{S_i\}, H)}{kT}}}{Z(H, T)} \\ &= \frac{(kT)^2}{Z(H, T)} \frac{\partial^2 Z(H, T)}{\partial H^2}. \end{aligned} \quad (3.55)$$

By using the equation above, the magnetic susceptibility can be reformulated as

$$\begin{aligned} \chi &= kT \frac{\partial}{\partial H} \left( \frac{1}{Z(H, T)} \frac{\partial Z(H, T)}{\partial H} \right) \\ &= \frac{kT}{Z(H, T)} \frac{\partial^2 Z(H, T)}{\partial H^2} - \frac{kT}{Z^2(H, T)} \left( \frac{\partial Z(H, T)}{\partial H} \right)^2 \\ &= \frac{[\langle m^2 \rangle] - [\langle m \rangle]^2}{kT}. \end{aligned} \quad (3.56)$$

This is the equation which states that the magnetic susceptibility can be measured from the fluctuations in the magnetization.

### 3.6.4 Mean-square disorder average local moment( $q$ )

The mean-square disorder average local moment indicates the magnetic order of the system. It is also called spin glass magnetization. The mean-square disorder average local moment can be calculated from

$$q \equiv [\langle S_i \rangle^2], \quad (3.57)$$

which is the overlap between two independent equilibrated configurations  $\{S_i^\alpha\}$  and  $\{S_i^\beta\}$  of the same disorder realization [10]. If the systems are construct from same set of interactions ( $J_{ij}$ ), the shape of domains should be very similar. For example, let the systems be the Ising model below critical temperature. The systems are ferromagnetic phase which the average magnetization can be up or down. The average magnetization of the systems can be difference but the domain wall should be very similar. In this case the mean-square disorder average local moment should not be zero. In other hand, if the temperature of the system is above the critical temperature, the systems are in paramagnetic phase which the zero average magnetizations and there is no domain wall. So the mean-square disorder average local moment should be zero. By using mean-square disorder average local moment, the similarity of systems can be calculated.

### 3.6.5 Binder cumulants( $U, g$ )

The Binder cumulant was introduced by Kurt Binder [18] to overcome the finite size effect. It is a quantity that is supposed to be invariant of the system sizes at criticality. The magnetization Binder cumulant [18] is defined by

$$U = 1 - \frac{[\langle m^4 \rangle]}{3[\langle m^2 \rangle]^2}. \quad (3.58)$$

The spin glass Binder cumulant [19, 20] is defined by

$$g = \frac{1}{2} \left( 3 - \frac{[\langle q^4 \rangle]}{[\langle q^2 \rangle]^2} \right). \quad (3.59)$$

By varying the size of the simulated model and away from critical point, the Binder cumulant from the difference system size are difference. However the Binder cumulants corresponding to different system sizes intersect at approximately certain

temperature, which is the critical temperature. This provides us a convenient and precise tool to estimate the value of the critical temperature.



ศูนย์วิทยทรัพยากร  
จุฬาลงกรณ์มหาวิทยาลัย

# CHAPTER 4

## SIMULATION PROCESS

The simulation processes and important parameters calculation are presented in this chapter.

### 4.1 State transition and Metropolis algorithm

This algorithm was proposed by Nicholas Metropolis in 1953 [21]. From canonical ensemble, the probability that the system can be in a particular state can be calculated from equations (2.2) and (2.3) as

$$\rho = \frac{e^{-\beta H(x,p)}}{Z_N(V,T)}. \quad (4.1)$$

The system transits from one state to other state in the phase space but it is limited by transition probability. The transition probability can be calculated from the state density of initial state and final state as

$$\begin{aligned} P(x \rightarrow x') &= \frac{\rho(x')}{\rho(x)} \\ &= \frac{e^{-\beta_{x'} H(X')}}{e^{-\beta_x H(X)}}. \end{aligned} \quad (4.2)$$

In Metropolis algorithm [21], the temperature in the initial state and final state are the same. The transition probability can be written as

$$\begin{aligned} P(x \rightarrow x') &= \frac{e^{-\beta H(X')}}{e^{-\beta H(X)}} \\ &= e^{-\beta(H(X')-H(X))} \\ &= \begin{cases} 1 & \text{if } H(X') - H(X) < 0 \\ e^{-\beta(H(X')-H(X))} & \text{if } H(X') - H(X) > 0. \end{cases} \end{aligned} \quad (4.3)$$

As the common of nature, the system always seeks for the lowest energy state if possible. This equation shows that if the future state has the energy lower than the initial state, the system always transits to the future state. But if the future state has the energy higher than the initial state, the probability of the transition is limited by equation (4.3). For a given temperature, there are the equilibrium states that the transition probability of transit to the higher energy and transit to the lower energy are equal. From this basic idea of the state transition, the Markov process can be constructed as follows.

1. Select a spin, either randomly or sequentially.
2. Calculate the transition probability  $P$ .
3. Compare  $P$  to a random number  $0 < z < 1$ .
4. Flip the spin if  $P > z$ , or use the initial state if  $P < z$ .
5. Use the final state to generate the value of any thermodynamic quantity to be averaged. Store this value.

It is important to be aware that any bias in the random number generator will introduce systematic errors into the results.

## 4.2 Simulation process

To simplify this model, the values of  $J_0$  in the equation have been set to

$$J_0 = 1.$$

And the degree of disorder, the value of  $J$ , is start from 0 to 2 with a increment 0.05, while  $\beta$  are chosen from difference temperatures.

To minimize the finite-size effect, the number of lattice site is set to be  $100 \times 100$ . The simulation process can be constructed as follows.

1. Setup the spin and interaction that have no disorder,  $J = 0$ .

2. Setup the magnetic interaction for each pair of the spin according to the distribution law.
3. Start metropolis algorithm to let the system achieve the equilibrium state by using 100000 MCS.
4. At the equilibrium state, collect the important data from every 10 MCS and calculate the average for 100 times.
5. Repeat step 2 and average the value over different set of magnetic interaction, using 100 sets of magnetic interaction.
6. Increase the width of the interaction and repeat the process until it reaches the target value.
7. Change the temperature and simulate again.

For a better speed, the simulation is run in cluster computer. The important parameters which can be calculated and collected in each temperature and disorder during the simulation process are energy, heat capacity, average magnetization, mean-square disorder average local moment and magnetic susceptibility.

### 4.3 Important parameters

#### 4.3.1 Energy( $E$ )

The energy of the system can be calculated from simulation by the summation over all the interactions between spins. By using the equation

$$H = - \sum_{\langle ij \rangle} J_{ij} S_i S_j, \quad (4.4)$$

the algorithm for energy calculation can be constructed.

### 4.3.2 Heat capacity( $C_V$ )

The heat capacity can be calculated after the energy data is completed. The heat capacity relates to the slope of the graph between energy and temperature. It can be written as

$$C_V = \frac{\partial[\langle E \rangle]}{\partial T}, \quad (4.5)$$

or the fluctuation in the energy which can be written as

$$C_V = \frac{[\langle E^2 \rangle] - [\langle E \rangle]^2}{T^2}. \quad (4.6)$$

From the equation 4.5, heat capacity can be calculated by the derivative of energy respect with temperature. In this algorithm, the energies in nearby temperatures must be found in order to calculate heat capacity which leads to increase of simulation time.

The algorithm that used in this thesis is constructed from equation 4.6. Heat capacity is calculated from the fluctuation in the energy at constant temperature. This algorithm is faster than the previous one since the simulations in nearby temperature is not used in the algorithm.

### 4.3.3 Average magnetization( $m$ )

The average magnetization can be calculated from simulation by sum over all spin and divided by number of spin sites. By using the equation

$$m = \frac{1}{N} \sum_{i=1}^N S_i, \quad (4.7)$$

the algorithm of average magnetization can be constructed.

### 4.3.4 Magnetic susceptibility( $\chi$ )

The magnetic susceptibility can be calculated after the average magnetization data is completed. The magnetic susceptibility relates to the slope of the average magnetization and applied magnetic field that can be written as

$$\chi = \frac{\partial[\langle m \rangle]}{\partial H}. \quad (4.8)$$

It is also related to the fluctuation in the average magnetization which can be written as

$$\chi = \frac{[\langle m^2 \rangle] - [\langle m \rangle]^2}{kT}. \quad (4.9)$$

From the equation 4.8, magnetic susceptibility can be calculated by the derivative of average magnetization with respect to external magnetic field. In this algorithm, the average magnetization in nearby external magnetic field must be found in order to calculate the average magnetization which leads to longer simulation time.

The algorithm that used in this thesis is constructed from equation 4.9. Magnetic susceptibility is calculated from the fluctuation in the average magnetization at constant temperature.

### 4.3.5 Mean-square disorder average local moment( $q$ )

The mean-square disorder average local moment can be calculated by[19, 20]

$$q = \frac{1}{N} \sum_i S_i^\alpha S_i^\beta, \quad (4.10)$$

where  $S_i^\alpha$  and  $S_i^\beta$  are independent equilibrated configurations but using the same set of magnetic interaction. So the mean-square disorder average local moment, for a given set of magnetic interaction, can be calculated from the equation 4.10 according to the following simulation processes:

1. Setup the replica system.
2. Simulate the replica system independently with the main system.
3. Calculate the mean-square disorder average local moment by using replica system and the main system according to 4.10.

### 4.3.6 Binder cumulant( $U, g$ )

The binder cumulant can be calculated by using the equations

$$U = 1 - \frac{[\langle m^4 \rangle]}{3[\langle m^2 \rangle]^2}, \quad (4.11)$$

$$g = \frac{1}{2} \left( 3 - \frac{[\langle q^4 \rangle]}{[\langle q^2 \rangle]^2} \right). \quad (4.12)$$



Both binder cumulants must be calculated from difference sizes in order to determine the critical temperatures. In this thesis, the size that be simulated are 10, 20, 30, 40, 50.



ศูนย์วิทยทรัพยากร  
จุฬาลงกรณ์มหาวิทยาลัย

# CHAPTER 5

## RESULTS AND DISCUSSIONS

The results from simulation and discussions are represented in this chapter. We have used the modified random bond Ising model with Gaussian distribution of magnetic interaction as described in the last chapter.

### 5.1 Simulation results

The results from the simulation process are shown in this section. The parameters that have been varied are temperature and degree of disorder  $J$ , after that the important parameters are calculated accordingly.

#### 5.1.1 Energy( $E$ )

In the Ising model, the average energy depends on the temperature. In the modified random-bond Ising model, the similar result is expected. The results from the simulation are shown in Figures 5.1 and 5.2.

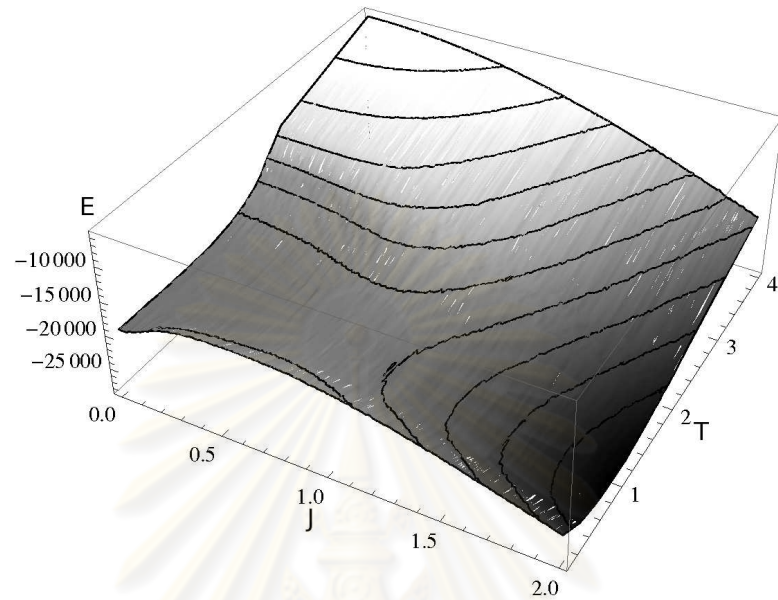


Figure 5.1: Energy as a function of temperature,  $T$ , and the width of the interaction distribution  $J$ .

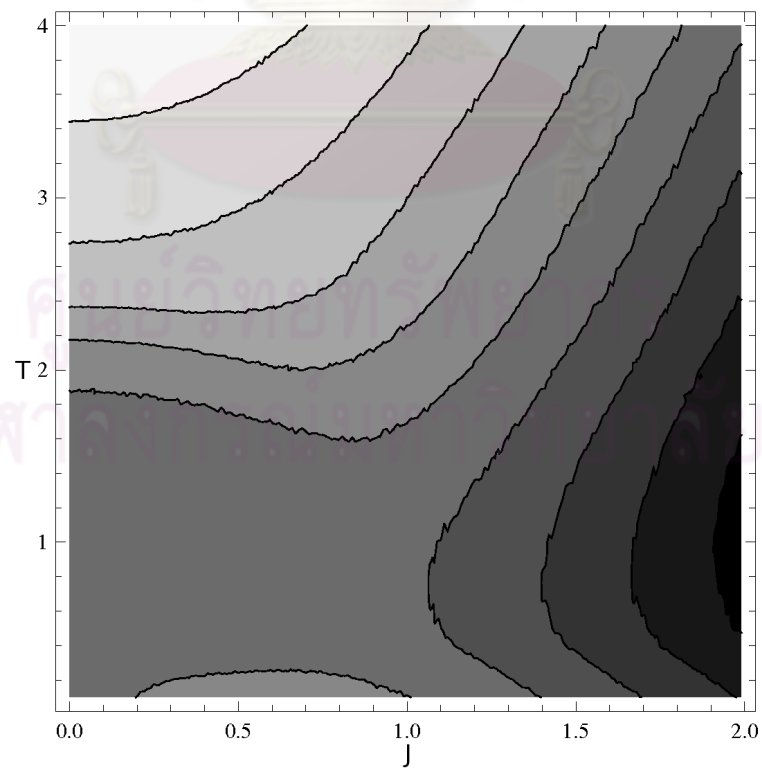


Figure 5.2: Contour plot of energy diagram as a function of temperature,  $T$ , and the width of the interaction distribution  $J$ .

It is shown that at  $J = 0$  the system becomes Ising model and the calculated energy from our results agree with that of the Ising model. At finite  $J$  the energy is also increase which similar to 2 dimensional Ising model except the  $T \leq 1$  region. At this region the energy decrease as the temperature increase until it reaches the minimum value. It is expected that at  $T \leq 1$  region the system is trapped in the local minima that it is not a true ground state. So the results in this region might not reflect the ground state properties. In other region, as the disorder increases the energy of the system reduces due to the interaction's distribution. Since 50% of the interactions are distributed in  $J_{ij} \geq 1$  region. The energy should decrease as the disorder increase.

### 5.1.2 Heat capacity ( $C_V$ )

The heat capacity can be calculated after the energy data is completed. From Figures 5.1 and 5.2, the areas that the energies increase rapidly with temperature will have the higher heat capacity, while the areas that the energies remain almost constant will have the lower heat capacity. The results from the simulation are shown in Figures 5.3 and 5.4.

ศูนย์วิทยทรัพยากร  
จุฬาลงกรณ์มหาวิทยาลัย

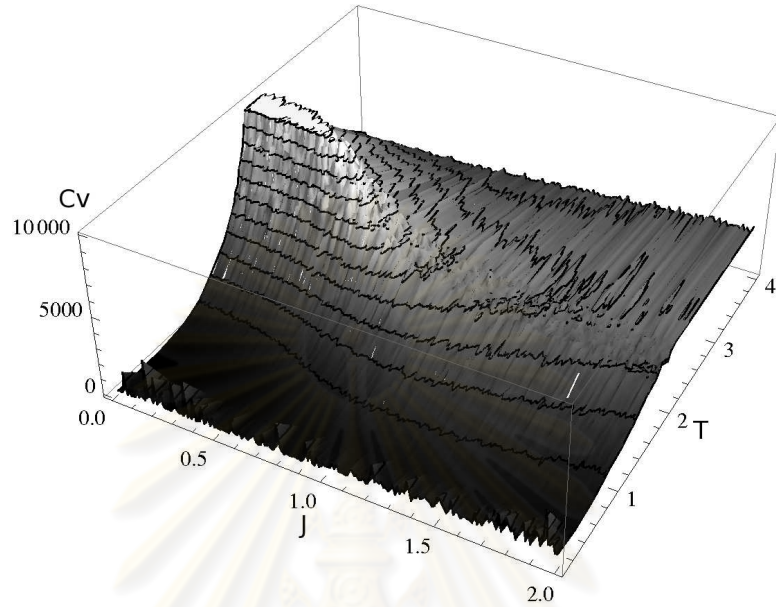


Figure 5.3: 3-D diagram of heat capacity  $C_V$  as a function of temperature,  $T$ , and the width of the interaction distribution  $J$ .

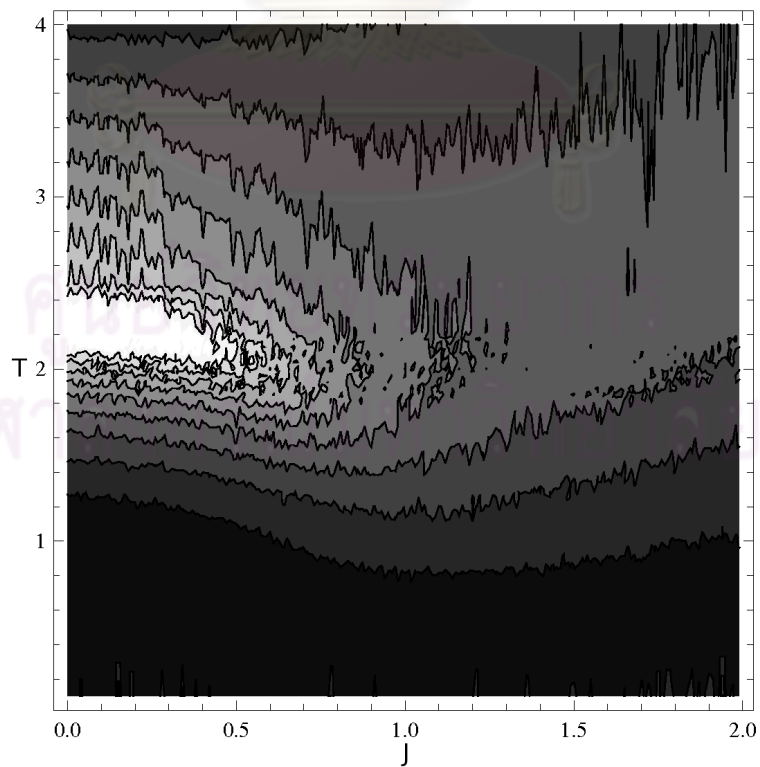


Figure 5.4: Contour plot of heat capacity  $C_V$  as a function of temperature,  $T$ , and the width of the interaction distribution  $J$ .

The areas that have high heat capacity from Figures 5.3 and 5.4 are the area that have a very steep slope in Figures 5.1 and 5.2 or have a very high fluctuation in Figure 5.1 and 5.2.

### 5.1.3 Average magnetization( $m$ )

The average magnetization indicates the magnetic phases of the system in the macroscopic scale. The average magnetization is calculated by summation of over all magnetization on every spin sites and then divide by the number of sites. The results from the simulation are shown in Figures 5.5 and 5.6. Without disorder,  $J = 0$ , the average magnetization is followed that of the 2 dimensional Ising model. The transition between ferromagnetic and paramagnetic is clearly being seen.

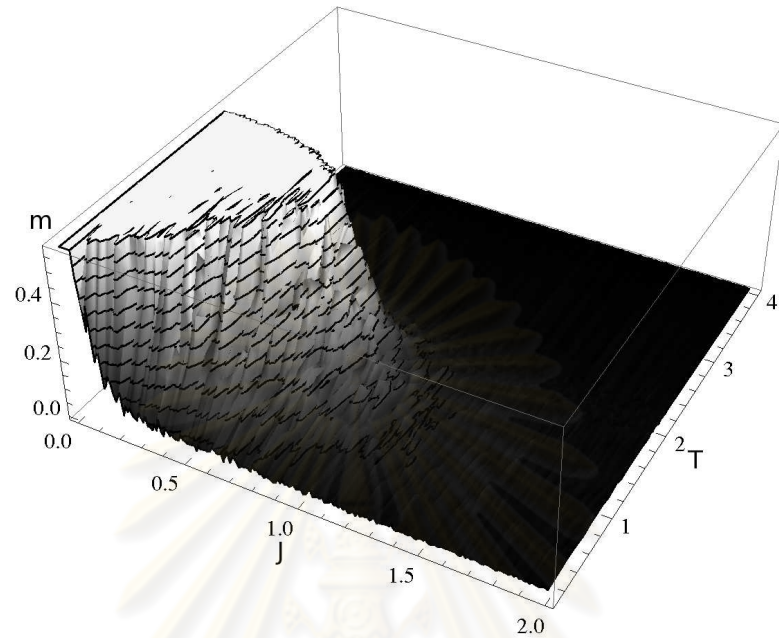


Figure 5.5: 3-D diagram of average magnetization  $m$  as a function of temperature,  $T$ , and the width of the interaction distribution  $J$ .

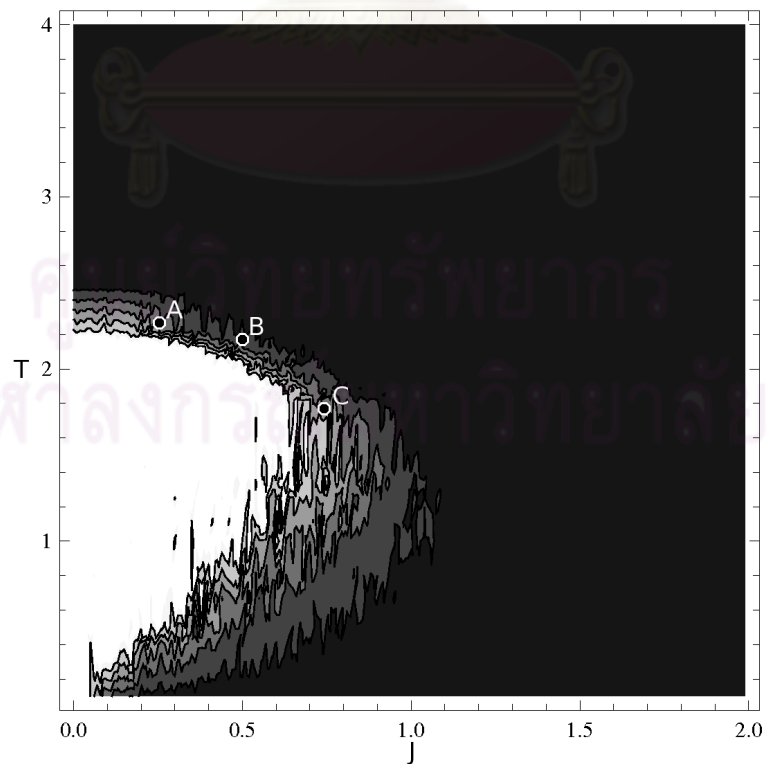


Figure 5.6: Contour plot of average magnetization  $m$  as a function of temperature,  $T$ , and the width of the interaction distribution  $J$ .

The average magnetization depends on the temperature and disorder. Without disorder, the system behaves in the same way as the 2 dimensional Ising model. While the disorder increases, the average magnetization decreases to zero. However the average magnetization is not enough in determining the spin glass phase since the spin glass phase and paramagnetic phase both have zero average magnetization. Points A, B and C correspond to the transition points obtained from Binder cumulant of magnetization.

#### 5.1.4 Magnetic susceptibility( $\chi$ )

The magnetic susceptibility can be calculated after the average magnetization data is completed. The magnetic susceptibility is plotted against temperature as can be seen from Figures 5.5 and 5.6.

The areas that have high magnetic susceptibility from Figures 5.7 and 5.8 are the area that have a very steep slope in Figures 5.5 and 5.6 or have a very high fluctuation in Figures 5.5 and 5.6.



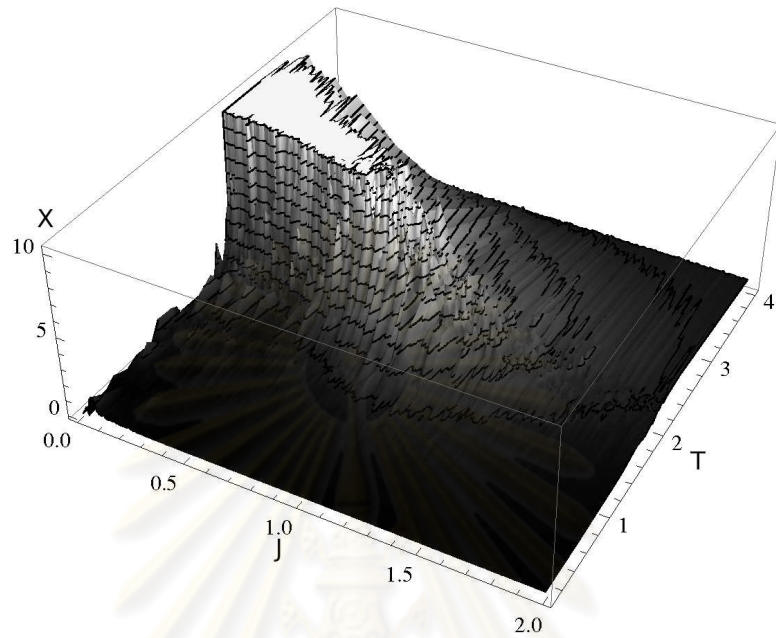


Figure 5.7: 3-D diagram of magnetic susceptibility  $\chi$  as a function of temperature,  $T$ , and the width of the interaction distribution  $J$ .

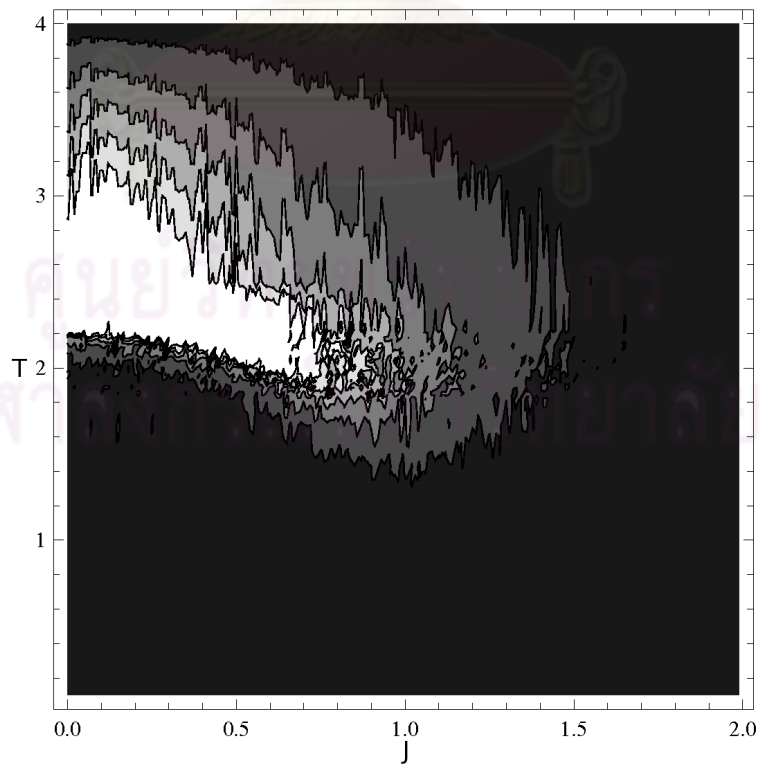


Figure 5.8: Contour plot of magnetic susceptibility  $\chi$  as a function of temperature,  $T$ , and the width of the interaction distribution  $J$ .

### 5.1.5 Mean-square disorder average local moment( $q$ )

The results from the simulation are shown in Figures 5.9 and 5.10. This parameter can be used to define the phase of the system similar to the average magnetization. It can also be used to measure the magnetization at microscopic scale.



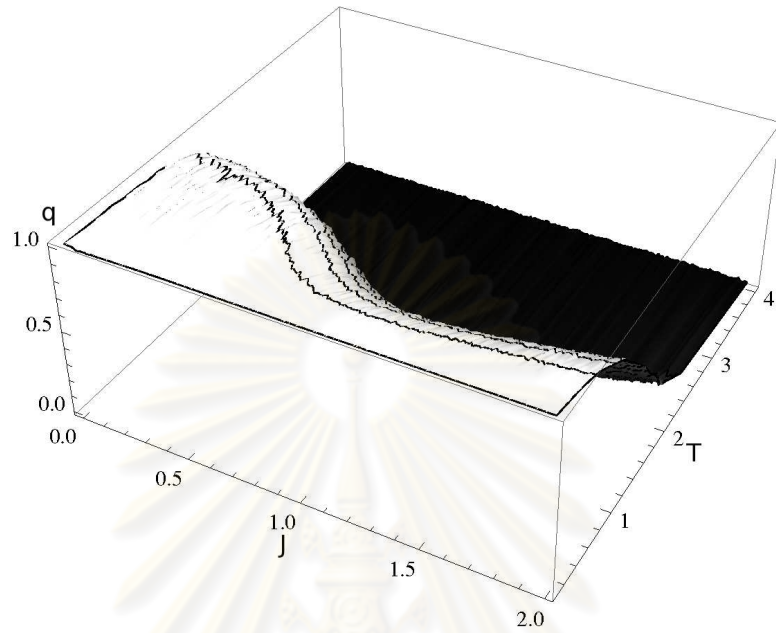


Figure 5.9: 3-D diagram of Mean-square disorder average local moment ( $q$ ) as a function of temperature,  $T$ , and the width of the interaction distribution  $J$ .

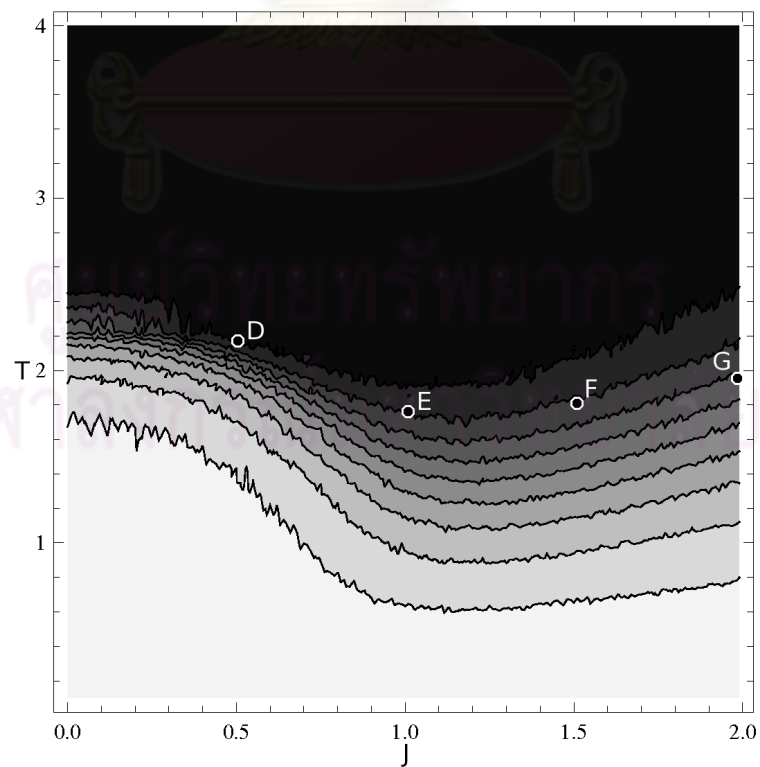


Figure 5.10: Contour plot of Mean-square disorder average local moment ( $q$ ) as a function of temperature,  $T$ , and the width of the interaction distribution  $J$ .

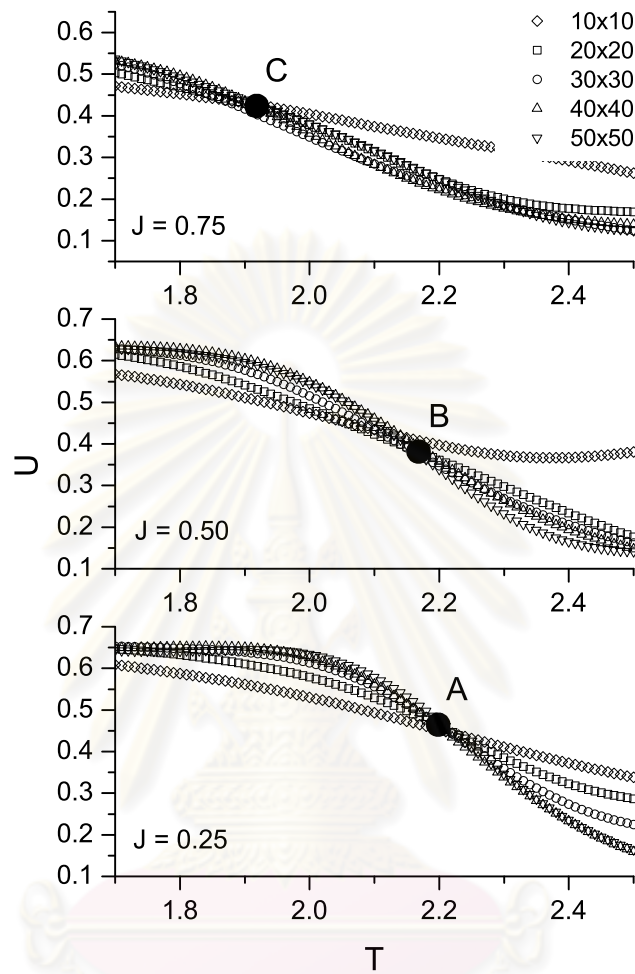


Figure 5.11: Magnetization Binder cumulant at  $J = 0.25$ ,  $J = 0.50$ ,  $J = 0.75$  at difference system size.

Points D, E, F and G refer to the transition points obtained from Binder cumulant of the spin glass magnetic moment.

### 5.1.6 Binder cumulant( $U, g$ )

The Binder cumulants of magnetization and spin glass magnetization at different degree of disorder are shown in Figures 5.11 and 5.12. In each Figure, the system size that has be simulated are 10, 20, 30, 40 and 50.

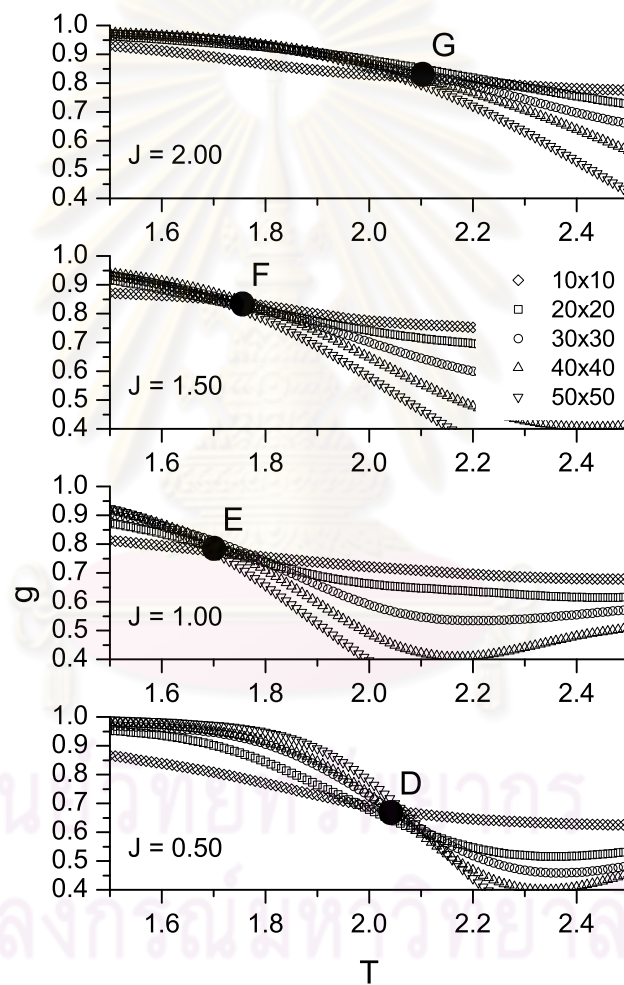


Figure 5.12: Spin glass Binder cumulant at  $J = 0.50$ ,  $J = 1.00$ ,  $J = 1.50$ ,  $J = 2.00$  at different system size.

From Figures 5.11 and 5.12, the intersection points in Binder cumulants agree with the result from the phase diagram that determined by  $m$  and  $q$ . These results indicate that the phase transition can be determined by Both Binder cumulants and magnetizations.

## 5.2 Phase diagram

The phase diagram of the modified random-bond Ising model can be determined by using the average magnetization and mean-square disorder average local moment. The phases can be categorized as follows.

1. paramagnetic if both  $m$  and  $q$  are zero.
2. ferromagnetic if both  $m$  and  $q$  are non-zero.
3. spin glass if  $q$  is non-zero but  $m$  is zero.

ศูนย์วิทยทรัพยากร  
จุฬาลงกรณ์มหาวิทยาลัย

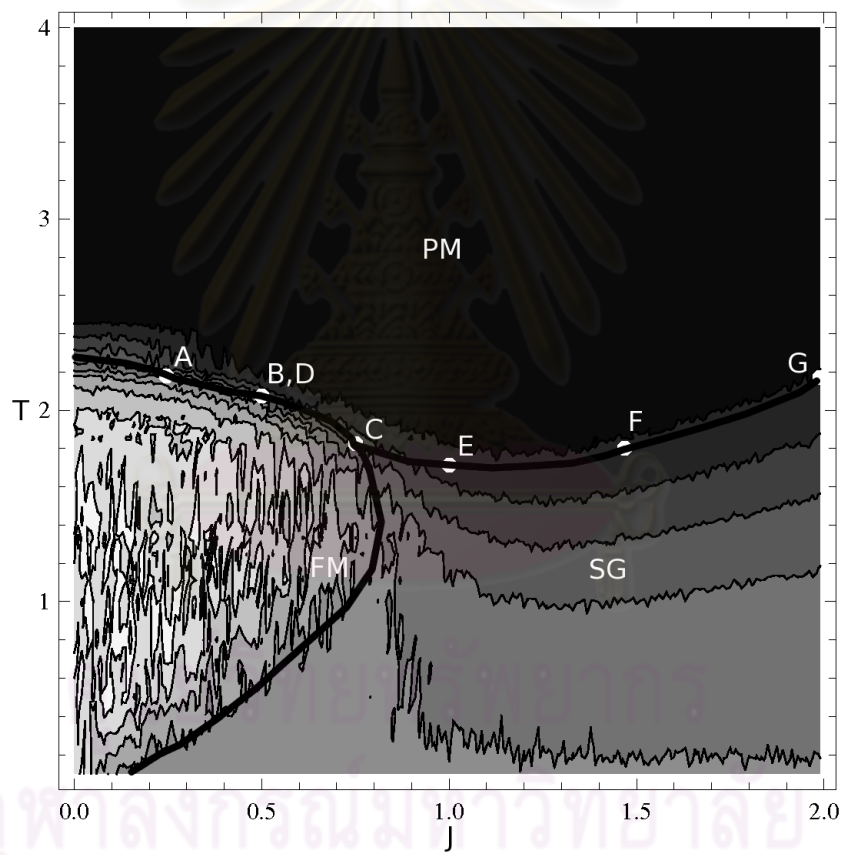


Figure 5.13: Phase diagram of modified random-bond Ising model.

The Figures 5.5, 5.6, 5.9, 5.10 and 5.13 show that these phase depends on temperature and disorder. The phase diagram that obtained from this model is difference from the one that has been used in [22]. In their results there are mixed phase between the spin glass phase and ferromagnetic phase which is difference from the modified random-bond Ising model. When compare with the result from [10], the phase diagrams are similar, expect that the slope of boundary between paramagnetic phase and spin glass phase from ours results is shallow than that of reference [10]. Also the boundary between ferromagnetic and spin glass phase from ours result depends on the temperature while the result from [10] does not. In Figures 5.3, 5.4, 5.7 and 5.8, the peak in those Figures occur in the same region which is paramagnetic phase. In 2 dimensional Ising model, these peaks are located at the phase transition line between ferromagnetic phase and ferromagnetic phase. But the result from modified random-bond Ising model shows that these peak are shifted from the phase boundary.

The transition from ferromagnetic phase to spin glass phase at low temperature occurs at lower disorder than high temperature. At low temperature and low disorder, most of the interactions are distributed in positive region. As the result most of the local spins try to align in same direction, but there are domain walls that occur when the disorder increase cause the average magnetization become zero, however the magnetic order is preserved in small scale.



# CHAPTER 6

## CONCLUSIONS

The main purpose of this work is to study the phase transition in modified random-bond Ising model. The modified random-bond Ising model is based on 2 dimensional Ising model with the interaction that is distributed according to the Gaussian distribution. The hypothesis is that adding another material to the system will cause the system to become distorted, as a result, the width of the interaction become wider.

From the simulation results, the average energy increases while the temperature increases except at  $T \leq 1$  region. The result in  $T \leq 1$  region might not represent the true properties of the ground state since the system is trapped in the local minimum. In other region, as the disorder increases the energy of the system reduces due to the interaction's distribution. Since 50% of the interactions are distributed in the  $J_{ij} \geq 1$  region. The energy should decrease as the disorder increases.

Phase diagram can be obtained by using the average magnetization ( $m$ ) and mean-square disorder average local moment ( $q$ ) and the Binder cumulants. Phase diagram obtained from parameters  $m$  and  $q$  is qualitatively agrees with the transition point obtained from the binder cumulants.

Peaks in heat capacity and magnetic susceptibility in 2 dimensional Ising model locate at the phase transition line between ferromagnetic phase and ferromagnetic phase. While the result from modified random-bond Ising model shows that these peaks are shifted from the phase boundary.

Transition from ferromagnetic phase to spin glass phase at low temperature occurs at lower disorder than high temperature. At low temperature and low disorder, most of the interactions are distributed in positive region. As the result most

of the local spins try to align in the same direction, but there are domain walls that occur when the disorder increases cause the average magnetization becomes zero, while there is magnetic order in small scale.



ศูนย์วิทยทรัพยากร  
จุฬาลงกรณ์มหาวิทยาลัย

# REFERENCES

1. Max Plank, On the law of distribution of energy in the normal spectrum, *Annalen der Physik*, 1 (1901): 719-737.
2. Ernest Ising, Contribution to the theory of ferromagnetism, *Zeitschrift fur physik*, (1925).
3. Lars Onsager, Crystal statistics. I. A two-dimensional model with an order-disorder transition, *Phys. Rev.* 65(1044): 117149
4. S. F. Edwards and P. W. Anderson, Theory of spin glasses, *J. Phys. F*, 5 (1975): 965.
5. W. Fan, K. Jungho and Y.J. Kim, Reentrant spin glass transition in  $LuFe_2O_{4-\delta}$ , arXiv:0712.1975v1 [cond-mat].
6. H.G. Katzgraber, D. Herisson, M. Oesth, P. Nordblad, A. Ito and H.A. Katori, Finite versus zero-temperature hysteretic behavior of spin glasses: Experiment and theory, *Phys. Rev. B*, 76 (2007): 092408.
7. L. Viana and A. J. Bray, Phase diagrams for dilute spin glasses, *J. Phys. C*, 18 (1985): 3037.
8. Mezard and G. Parisi, The Bethe lattice spin glass revisited, *Eur.Phys. J. B*, 20 (2001): 217.
9. S. Franz and M. Leone, Replica bounds for optimization problems and diluted spin systems, *J. Stat. Phys*, 111 (2003): 535.
10. D. Sherrington and S. Kirkpatrick, Solvable model of a spin-glass, *Phys. Rev. Lett*, 35 (1975): 1792.
11. M. Mezard, G. Parisi and M.A. Virasoro, *Spin glass theory and beyond*, Singapore, World Scientific, 1987.

12. G. Parisi, *Field theory, disorder and simulation*, Singapore, World Scientific, 1992.
13. K. H. Fischer, Static properties of spin glasses, *Phys. Rev. Lett.*, 34 (1975): 1438.
14. M. Picco, A. Honecker and P. Pujol, Strong disorder fixed points in the two-dimensional random-bond Ising model, *JSTAT*, (2006): P09006.
15. I. Morgenstern, Numerically exact solvable random-bond Ising model, *Z. Phys. B*, 41 (1981): 147.
16. N.G. Fytas and A. Malakis, Phase Diagram of the 3D Bimodal Random-Field Ising Model, *Eur.Phys. J. B*, 61 (2008): 111.
17. A. G. Schins, A. F. Arts and H. W. de Wijn, Domain growth by aging in nonequilibrium two-dimensional random Ising systems, *Phys. Rev. Lett*, 70 (1993): 2340.
18. K. Binder, Finite size scaling analysis of Ising model block function, *Z. Phys. B*, 43 (1981): 119.
19. J. Houdayer, A. K. Hartmann, Low-temperature behavior of two-dimensional Gaussian Ising spin glasses, *Phys. Rev. B*, 70 (2004): 014418.
20. R.N. Bhatt and A.P. Young, Numerical studies of Ising spin glasses in two, three, and four dimensions, *Phys. Rev. B*, 37 (1988): 5606.
21. N. Metropolis, A. W. Rosenbluth, M. N. Rosenbluth and A. H. Teller, Equation of state calculations by fast computing machines, *J. Chem. Phys.*, 21 (1953): 6.
22. S. Niidera, S. Abiko and F. Matsubara, Phase diagram of a dilute ferromagnet model with antiferromagnetic next-nearest-neighbor interactions, *Phys. Rev. B*, 72 (2005): 214402.
23. K. Hukushima and K. Nemoto, Exchange Monte Carlo method and application to spin glass simulation, *J. Phys. Soc. Jpn.*, 65 (1996): 1604.

24. Helmut G. Katzgraber, Simon Trebst, David A. Huse and Matthias Troyer, Feedback-optimized parallel tempering Monte Carlo, *J. Stat. Mech.*, (2006): P03018.
25. S. Trebst, D. A. Huse, and M. Troyer, Optimizing the ensemble for equilibration in broad-histogram Monte Carlo simulations, *Phys. Rev. E*, 70 (2004): 046701.



ศูนย์วิทยทรัพยากร  
จุฬาลงกรณ์มหาวิทยาลัย



# APPENDICES

ศูนย์วิทยทรัพยากร  
จุฬาลงกรณ์มหาวิทยาลัย

# APPENDIX A

## USING MPI

This appendix involves with basic idea of cluster computing and using cluster computer.

### A.1 Basic MPI concept

MPI is a language-independent communications protocol used to program parallel computers. Both point-to-point and collective communication is supported. MPI is a message-passing application programmer interface, together with protocol and semantic specifications for how its features must behave in any implementation. MPI's goal are high performance, scalability and portability. MPI remains the dominant model used in high-performance computing today.

#### A.1.1 Parallel computational models

A computational model is a conceptual view of what types of operations are available to the program. It does not include the specific syntax of a particular programming language or library and it is independent of the underlying hardware that supports it. The effectiveness of such an implementation depends on the gap between the model and the machine.

Parallel computational models form a complicated structure. They can be differentiated along multiple axes. The picture is made confusing by the fact that software can provide an implementation of any computational model on any hardware.

#### Data parallelism

Although parallelism occurs in many places and at many levels in a modern computer, one of the first places it was made available to the programmer was in vector processors. Indeed, the vector machine began the current age of supercomputing.

The vector machine's notion of operating on an array of similar data item in parallel during a single operation has been extended to include the operation of the whole programs on collections of data structures. The parallelism need not necessarily processed instruction by instruction in lock step for it to be classified as data parallel. Data parallelism is now more a programming style than a computer architecture.

### **Shared memory**

Parallelism that is not determined implicitly by data independence but is explicitly specified by the programmer is control parallelism. One simple model of control parallelism is the shared-memory model, in which each processor has access to all of a single, shared address space at the usual level of load and store operations. Coordination of access to locations manipulated by multiple processes is done by some form of locking, although high-level language may hide the explicit use of locks. A variation on the shared-memory model occurs when processes have both a local memory (accessible only one process) and also share a portion of memory (accessible by some or all of the other processes).

### **Message passing**

The message-passing model posits a processes that have only local memory but are able to communicate with other processes by sending and receiving messages. It is a defining feature of the message-passing model that data transfer from the local memory of one process to the local memory of another requires operations to be performed by both processes.

### **Remote memory operations**

Halfway between the shared-memory model, where processes access memory without knowing whether they are triggering remote communication at the hardware level and the message-passing model, where both the local and remote processes must participate, is the remote memory operation model. Active messages are



often used to facilitate remote memory, which can be thought of as part of the active-message model. Such remote memory copy operations are exactly the "one-sided" sends and receives unavailable in the message-passing model.

### **Threads**

Early forms of the shared-memory model provided processes with separate address spaces, which could obtain shared memory through explicit memory operations. The more common version of the shared-memory now specifies that all memory is shared. This allows the model to be applied to multi-threaded systems in which a single process (address space) has associated with it several program counters and execution stack. Since the model allows fast switching from one thread to another and requires no explicit memory operations. The difficulty imposed by the thread model is that any "state" of the program defined by the value of program variables is shared by all threads simultaneously.

### **Combined models**

Combinations of the above models are also possible, in which some clusters of processes share memory with one another but communicate with other cluster via message passing, or in which processes may be multithreaded yet not share memory with one another.

## **A.1.2 Advantages of the Message-Passing Model**

### **Universality**

The message-passing model fits well on separate processors connect by a communication network. Thus, it matches the hardware of most of today's parallel super-computer, as well as the workstation networks that are beginning to compute with them. Where the machine supplies extra hardware to support a shared-memory model, the message-passing model can take advantage of this hardware to speed data transfer.

## **Expressivity**

Message passing has been found to be a useful and complete model in which to express parallel algorithms. It provides the control missing from the data-parallel and compiler-based models. Some find its anthropomorphic flavor useful in formulating a parallel algorithm. It is well suited to adaptive, self-scheduling algorithms and to programs that can be made tolerant of the imbalance in process speeds found in shared networks.

## **Ease of debugging**

Debugging of parallel programs remains a challenging research area. While debuggers for parallel programs are perhaps easier to write for the shared-memory model, it is arguable that the debugging process itself is easier in the message-passing paradigm. This is because one of the most common causes of error is unexpected overwriting of memory. The message-passing model, by controlling memory reference more explicitly than any of the other models, makes it easier to locate erroneous memory reads and writes.

## **Performance**

The most compelling reason that message passing will remain a permanent part of the parallel computing environment is performance. As modern CPUs have become faster, management of their caches and the memory hierarchy in general has become the key to getting the most out of them. Message passing provides a way for the programmer to explicitly associate specific data with processes and thus allow the compiler and cache-management hardware to function fully. Indeed, one advantage distributed-memory computers have over even the largest single processor machines is that they typically provide more memory and more cache. Memory-bound applications can exhibit super-linear speedups when ported to such machines. And even on shared-memory computers, use of the message-passing model can improve performance by providing more programmer control of data locality in the memory hierarchy.

This analysis explains why message passing has emerged as one of the more widely used paradigms for expressing parallel algorithms. Although it has shortcomings, message passing comes closer than any other paradigm to being a standard approach for the implementation of parallel applications.

## A.2 Setup the MPI

Before any MPI programs can be executed, the Local Area Multi-computer (LAM) run-time environment must be launched. This is typically called "booting LAM". A successfully boot process creates a an instance of the LAM run-time environment commonly referred to as the "LAM universe".

LAM's run-time environment can be executed in many different environments. It can be run interactively on a cluster of workstations even on a single workstation or LAM can be run in production batch scheduled systems.

When using *rsh* or *ssh* to boot LAM, a test file listing hosts on which to launch the LAM run-time environment is necessary for booting the LAM. For example:

```
node1.cluster.example.com user=username
node2.cluster.example.com user=username
node3.cluster.example.com cpu=2 user=username
node4.cluster.example.com cpu=2 user=username
```

Four nodes are specified in the above example by listing their IP hostnames. Note also the "cpu=2" that follows the last two entries. This tells LAM that these machines each have two CPU's available for running MPI programs. It is important to note that the number of CPU's specified hereh has no correlation to the physical number of CPUs in the machine. It is simply a convenience mechanism telling LAM how many MPI processes will be launch on that node.

### A.2.1 The lamboot command

The lamboot command is used to launch the LAM run-time environment. For each machinae listed in the boot schema, the following condition must be met for LAM's run-time environment to be bootes correctly:

- The machine must be reachable and operational.
- The user must be able to non-interactively execute arbitrary commands on

the machine.

- The LAM executables must be locatable on that machine, using the user's shell search path.
- The user must be able to write to the LAM session directory.
- The shell's start-up scripts must not print anything on standard error.
- All machines must be able to resolve the fully-qualified domain name (FQDN) of all the machines be booted.

### Using *ssh* with LAM

While *rsh* is the default remote transport agent that LAM uses to spawn the LAM daemons, it can be changed to other agents such as *ssh*. *ssh* is a popular choice because of the added security. And since *ssh* can pass AFS tokens, it presents an attractive, highly secure, yet fully AFS-authenticated method, for invoking LAM.

The remote shell agent that was specified at configure can be overridden with the LAMRSH environment variable. Setting this environment variable before invoking *recon*, *lamboot*, or any other LAM executable will force LAM to use that remote shell program instead. For example, using a Bourne shell or some other *sh* derivative:

```
% LAMRSH="ssh -x"
```

```
% export LAMRSH
```

Or, using the C shell or some *sh* derivative:

```
% setenv LAMRSH "rsh -x"
```

### Making *ssh* not ask for password

Normally, when using *ssh* to connect to a remote host, it will prompt for a password. However, in order for *lamboot* and *recon* to work properly, remote nodes are needed to be executed jobs without typing in a password. In order to do this, RSA or DSA authentication will be needed to be set up.

The first thing that must be done is generate an DSA key pair use with

ssh-keygen:

```
% ssh-keygen -t dsa
```

Accept the default value for the file in which to store the key ( $\$/HOME/\.ssh/id\_dsa$ ) and other a pass-phrase for keypair. Next, copy the  $\$/HOME/\.ssh/id\_dsa.pub$  file generated by *ssh-keygen* to

```
%cd $HOME/\.ssh
```

```
%cp id\_dsa.pub authorized\_keys
```

In order for DSA authentication to work the  $\$/\.ssh$  directory must be in home directory in all the machines are running LAM on. If not, the  $\$/\.ssh$  directory must be copied to home directory on all LAM nodes. However, when ssh to a remote host, the DSA pass-phrase still be asked. This is where the *ssh-agent* program comes in. It allow to type in DSA pass-phrase once and then have all successive invocations of *ssh* automatically authenticate against the remote host. To start up the *ssh-agent*, type:

```
% eval 'ssh-agent'
```

Once the *ssh-agent* is running, the pass-phrase can be enter by running the *ssh-add* command:

```
% ssh-add $HOME/\.ssh/id\_dsa
```

At this point, if *ssh* to a remote host that has the same  $\$/HOME/\.ssh$  directory as local one, a password should not be prompted.

Once all of these condition are met, the *lamboot* command is used to launch the LAM runtime environment. For example:

```
shell$ lamboot -v -ssi boot hostfile
```

The parameters passed to *lamboot* in the example above are as follows:

- -v: Make *lamboot* be slightly verbose.
- -ssi boot rsh: Ensure that LAM use the *rsh/ssh* boot module to boot the LAM universe. Typically, LAM chooses the right boot module automatically and therefore this parameter is typically necessary.
- hostfile: Name of the boot schema file.

Common cause of failure with the *lamboot* command include (but not limited to):

- User does not have permission to execute on the remote node. This typically involves setting up a `$HOME/.rhosts` file if using `rsh`, or properly configured `ssh` keys if using `ssh`.
- The first time a user uses `ssh` to execute on a remote node, `ssh` typically prints a warning to the standard error. LAM will interpret this as a failure. If this happens, `lamboot` will complain that something unexpectedly appeared on `stderr`, and abort. One solution is to manually `ssh` to each node in the boot schema once in order to eliminate the `stderr` warning, and then try `lamboot` again. Another is to use the `boot_rsh_ignore_stderr` SSI parameter.

### A.2.2 The `lamnodes` command

An easy way to see how many nodes and CPUs are in the current LAM universe is with the `lamnodes` command. For example, with the LAM universe that was created from the boot schema in section above, running the `lamnodes` command would result in the following output:

```
shell$ lamnodes
n0 node1.cluster.example.com:1:origin,this_node
n1 node2.cluster.example.com:1:
n2 node3.cluster.example.com:2:
n3 node4.cluster.example.com:2:
```

The "n" number on the far left is the LAM node number. For example, "n3" uniquely refers to node4. Also note the third column, which indicates how many CPUs are available for running processes on that node. In this example, there are total of 6 CPUs are available for running processes. This information is from the "cpu" key that was used in the hostfile, and is helpful for running parallel process. The "origin" notation indicates which node `lamboot` was executed from. "this\_node" indicates which node `lamnodes` is running on.

### A.2.3 Compiling MPI programs

Note that it is not necessary to have LAM booted to compile MPI program.

Compiling MPI programs can be a complicated process:

- The same compilers should be used to compile/link user MPI programs as were used to compile LAM itself.

- Depending on the specific installation configuration of LAM, a variety of -I, -L, -l flag and possibly others may be necessary to compile and/or link user MPI program.

LAM/MPI provides "wrapper" compilers to hide all of this complexity. These wrapper compilers simply add the correct compiler/linker flags and then invoke the underlying compiler to actually perform the compilation/link. As such, LAM's wrapper compilers can be used just like "real" compilers. The wrapper compilers are named mpicc (for C programs), mpiCC and mpic++ (for C++ programs) and mpif77 (for Fortran programs).

### A.3 Running the MPI

The mpirun and mpiexec commands are used for launching parallel MPI programs and the mpitask command can be used to provide crude debugging support. The lamclean command can be used to completely clean up a failed MPI program.

#### A.3.1 The MPI command

The mpirun command has many different options that can be used to control the execution of a program in parallel. The simplest way to launch the program across all CPUs listed in the boot schema is:

```
shell$ mpirun C hello
```

The C option means "launch one copy of hello on every CPU that was listed in the boot schema". The C notation is therefore convenient shorthand notation for launching a set of processes across a group of SMPs.

Another method for running in parallel is:

```
shell$ mpirun N hello
```

The N option has a different meaning than C - it means "launch one copy of hello on every node in the LAM universe". Hence, N disregards the CPU count. This can be useful for multi-threaded MPI programs.

Finally, to run an absolute number of processes regardless of how many CPUs or nodes are in the LAM universe:

```
shell$ mpirun -np 4 hello
```

This runs 4 copies of hello. LAM will "schedule" how many copies of hello will be run in a round-robin fashion on each node by how many CPUs were listed in

the boot schema file. For example, on the LAM universe that be shown previously, the following would be launched:

- 1 hello would be launched on n0 (named node1)
- 1 hello would be launched on n1 (named node2)
- 2 hello would be launched on n2 (named node3)

Note that any number can be used - if a number is used that is greater than how many CPUs are in the LAM universe, LAM will "wrap around" and start scheduling starting with that first node again. For example, using `-np 10` would result in the following schedule:

- 2 hello on n0 (1 from the first pass and then a second from the "wrap around")
- 2 hello on n1 (1 from the first pass and then a second from the "wrap around")
- 4 hello on n2 (2 from the first pass and then a second from the "wrap around")
- 2 hello on n3

The `mpirun(1)` man page contains much more information on `mpirun` and the option available.

### A.3.2 The `mpiexec` command

The MPI-2 standard recommends the use of `mpiexec` for portable MPI process startup. In LAM/MPI, `mpiexec` is functionally similar to `mpirun`. Some option that are available to `mpirun` are not available to `mpiexec` and vice-versa. The end result is topically the same, however both will launch parallel MPI program.

That being said , `mpiexec` offers more convenient access in three cases:

- Running MPMD programs.
- Running heterogeneous programs.



- Running "one-shot" MPI program

The general syntax for `mpiexec` is:

```
shell$ mpiexec <global_options> <cmd1> : <cmd2> : ...
```

### Running MPMD programs

For example, to run a manager/worker parallel program, where two different executables need to be launched:

```
shell$ mpiexec -n 1 manager : worker
```

This runs one copy of manager and one copy of worker for every CPU in the LAM universe.

### Running heterogeneous programs

Since LAM is a heterogeneous MPI implementation, it supports running heterogeneous MPI programs. Although this can be somewhat complicated to setup, the `mpiexec` command can be helpful in actually running the resulting MPI job.

### "One-shot" MPI programs

In some cases, it seems like extra work to boot a LAM universe, run a single MPI job, and then shut down the universe. Batch jobs are good examples of this since only one job is going to be run, `mpiexec` provides a convenient way to run "one-shot" MPI jobs.

```
shell$ mpiexec -machinefile hostfile hello
```

This will invoke `lamboot` with the boot schema named "hostfile", run the MPI program `hello` on all available CPUs in that resulting universe, and then shut down the universe with the `lamhalt` command.

### A.3.3 The `mpitask` command

The `mpitask` command is analogous to the sequential Unix command `ps`. It shows the current status of the MPI programs being executed in LAM universe and displays primitive information about what MPI function each process is currently

executing. Note that in normal practice, the `mpimsg` command only gives an snapshot of what messages are flowing between MPI processes and therefore is usually only accurate at that single point in time. To really debug message passing traffic, use a tool such as message passing analyzer or parallel debugger. `mpitask` can be run from any node in the LAM universe.

### A.3.4 The `mpiclean` command

The `lamclean` command completely removes all running programs from the LAM universe. This can be useful if a parallel job crashes and/or leaves state in the LAM runtime environment. It is usually run with no parameter:

```
shell$ lamclean
```

`lamclean` is typically only necessary when developing/debugging MPI application, Correct MPI programs should terminate properly, clean up all their message, etc.

## A.4 Shutting down the LAM universe

When finished with the LAM universe, it should be shut down with `lamhalt` command:

```
shell$ lamhalt
```

In most cases, this is sufficient to kill all running MPI processes and shut down the LAM universe.

However, in some rare condition, `lamhalt` may fail. For example, if any of the nodes in the LAM universe crashed before running `lamhalt`, `lamhalt` will likely timeout and potentially not kill the entire LAM universe. In this case, the `lamwipe` command will be needed to use to guarantee that the LAM universe has shut down properly:

```
shell$ lamwipe -v hostfile
```

where `hostfile` is the same boot schema that was used to boot LAM. `lamwipe` will forcibly kill all LAM/MPI processes and terminate the LAM universe. This is a slower process than `lamhalt` and is typically not necessary.

## APPENDIX B

# PARALLEL TEMPERING

The complex systems generally have numerous local minima which are separated from each others by energy barriers. The characteristic time in which the system can escape from a local minimum increases rapidly as temperature decreases. To overcome this problem, the algorithm is designed by Koji Hukushima and Koji Nemoto in 1996 [23]. Parallel tempering treats a compound system which consists of  $M$  replicas of the system. The temperature attributed to each replica is distributed in a range including both high and low temperature phases. The  $m$ -th replica, described by common hamiltonian  $H(X)$ , is associated with inverse temperature  $\beta_m$  (for convenience  $\beta_m < \beta_{m+1}$ ). A state of this extended ensemble is specified by  $\{X\} = \{X_1, X_2, \dots, X_M\}$ .

$$Z = \prod_{m=1}^M Z(\beta_m),$$

where  $Z(\beta)$  is the one for the original system. For a set of temperature  $\{\beta\}$  given, the probability distribution of finding  $\{X\}$  becomes

$$P(\{X, \beta\}) = \prod_m P_{eq}(X_m, \beta_m),$$

where

$$P_{eq}(X, \beta) = \frac{e^{-\beta H(X)}}{Z(\beta)} \quad (\text{B.1})$$

In constructing a Markov process for parallel tempering, a transition matrix  $W(X, \beta_m | X', \beta_n)$  which is a probability of exchange configurations of the  $n$ -th and  $m$ -th replicas must be introduced. In order to keep the system remains at equilibrium. it is sufficient to impose the detailed balance condition on the transition matrix:

$$\begin{aligned} & P(\dots; X, \beta_m; \dots; X', \beta_n; \dots) W(X, \beta_m | X', \beta_n) \\ &= P(\dots; X', \beta_m; \dots; X, \beta_n; \dots) W(X', \beta_m | X, \beta_n). \end{aligned}$$

From (B.1) it can be written as

$$\frac{W(X, \beta_m | X', \beta_n)}{W(X', \beta_m | X, \beta_n)} = \exp(-\Delta),$$

where

$$\Delta = (\beta_n - \beta_m)(H(X) - H(X')).$$

Therefore the replica-exchange part of transition probability can be expressed as

$$W(X, \beta_m | X', \beta_n) = \begin{cases} 1 & \text{if } \Delta < 0 \\ e^{-\Delta} & \text{if } \Delta > 0 \end{cases}$$

if the metropolis method have been adopted.

For the actual Monte Carlo procedure, the following two steps are performed alternately:

1. Each replica is simulated simultaneously and independently as canonical ensemble for a few Monte Carlo steps by using a standard Monte Carlo method.
2. Exchange of two configurations  $X_m$  and  $X_n$ , is tried and accepted with the probability  $W(X_m, \beta_m | X_n, \beta_n)$ .

The canonical expectation value of a physical quantity  $A$  is measured as follows:

$$\langle A \rangle_m = \frac{1}{N_{mcs}} \sum_{t=1}^{mcs} A(X_m(t)).$$

Another expression can be obtained when the exchange procedure mentioned above is regarded as for temperature instead of configurations, of a pair of replicas are to be exchanged. The the above quantity is expressed as

$$\langle A \rangle_\beta = \frac{1}{N_{mcs}} \sum_{t=1}^{N_{mcs}} \sum_{m=1}^M A(\tilde{X}_m(t)) \delta_{\beta, \beta_m(t)},$$

where the time-dependent inverse temperature  $\beta_m(t)$  and the configuration  $\tilde{X}_m$  are introduced in this temperature-exchange scheme. Note that both schemes are completely equivalent to one another. The two schemes can be chosen in actual implementation of the present method.

## B.1 Feedback-optimized temperature

In parallel tempering,  $M$  non-interacting replicas of the system are simultaneously set at a range of temperatures  $\{T_1, T_2, \dots, T_M\}$ . In order to maximize the number of statistically independent visits at low temperatures, the number of round-trips between the lowest and the highest temperature,  $T_1$  and  $T_M$  respectively, must be maximized for each replicas. The rate of round-trips of a replica strongly depends on the simulated statistical ensemble, that is the choice of temperature points  $\{T_1, T_2, \dots, T_M\}$  in the parallel tempering simulation. Helmut G. Katzgraber, Simon Trebst, David A. Huse and Matthias Troyer propose an algorithm that systematically optimizes the simulated temperature set to maximize the number of round-trips between the two extremal temperature for each replica [24]. By using geometric progression, the intermediate temperatures between the temperature range  $\{T_1, T_M\}$  can be computed via

$$T_k = T_1 \prod_{i=1}^{k-1} R_i, R_i = \sqrt[M-1]{\frac{T_M}{T_1}}.$$

The geometric progression peaks the number of temperatures around temperature  $T_1$  where a slower relaxation is assumed. For a given temperature set, the diffusion of a replica can be measured through temperature space by adding a label "up" or "down" to the replica that indicates which of the two extremal temperatures,  $T_1$  or  $T_M$  respectively, the replica has visited most recently. The label of a replica changes only when the replica visits the opposite extreme. For instance, the label of a replica with label "up" remains unchanged if the replica returns to the lowest temperature  $T_1$ , but change to "down" upon its first visit to  $T_M$ . For each temperature point in the temperature  $\{T_i\}$ , two histograms  $n_{up}(T_i)$  and  $n_{down}(T_i)$  must be recorded. If a replica has not yet visited either of the two extremal temperature, neither of the histograms must be incremented. This allow to evaluate for each temperature point the fraction of replica which have visited one of the two extremal temperature most recently as

$$f(T_i) = \frac{n_{up}(T_i)}{n_{up}(T_i) + n_{down}(T_i)}. \quad (\text{B.2})$$

The labeled replicas define a steady-state current  $j$  from  $T_1$  to  $T_M$  that is independent of the temperature. Assume that  $T$  is a continuous variable, independent

of the temperature points in the current temperature set. The current  $j$  can be determined to first order in the derivative as

$$j = D(T)\eta(T)\frac{df}{dT}, \quad (\text{B.3})$$

where  $D(T)$  is the local diffusivity at temperature  $T$  and the derivative  $df/dT$  is estimated by a linear regression based on the measurements in (B.2);  $\eta(T)$  is a density distribution indicating the probability for a replica to reside at temperature  $T$ .  $\eta(T)$  can be approximated with a step-function  $\eta(T) = C/\Delta T$ , where  $\Delta T = T_{i+1} - T_i$  is the length of the temperature interval around temperature  $T_i < T < T_{i+1}$  for the current temperature set. The normalization constant  $C$  is chosen such that

$$\int_{T_1}^{T_M} \eta(T)dT = C \int_{T_1}^{T_M} \frac{dT}{\Delta T} = 1. \quad (\text{B.4})$$

Rearranging (B.3) gives a simple measure of the local diffusivity  $D(T)$  of a replica at temperature  $T$

$$D(T) \sim \frac{\Delta T}{df/dT},$$

where the normalization constant  $C$  has been dropped and the current  $j$  which is constant for any specific choice of temperature set.

To increase the efficiency of the algorithm, the current  $j$  in temperature space is maximized by varying the simulated temperature set  $\{T_i\}$  and thus varying the probability distribution  $\eta(T)$  between the two extremal temperatures,  $T_1$  and  $T_M$ , which are not changed. In [25] it has been shown that the optimal probability distribution  $\eta^{opt}(T)$  is inversely proportional to the square root of the local diffusivity  $D(T)$ :

$$\eta^{opt}(T) \propto \frac{1}{D(T)}.$$

For the optimal distribution of temperature points the fraction  $f^{opt}(T)$  then decays as

$$\frac{df^{opt}}{dT} = \eta^{opt}(T) \propto \frac{1}{\Delta T^{opt}},$$

which implies that for any given temperature interval  $\Delta T = T_{i+1} - T_i$  of the optimal temperature set the fraction has a constant decay

$$\Delta f^{opt} = f^{opt}(T_i) - f^{opt}(T_{i+1}) = 1/(M - 1),$$

where  $M$  is the number of replicas.

After measuring the diffusion of replicas for given temperature set an improved probability distribution  $\eta'(T)$  is found as

$$\eta'(T) = \frac{C'}{\delta T'} = C' \sqrt{\frac{1}{\Delta T} \frac{df}{dT}},$$

where the normalization constant  $C'$  is again chosen so that the normalization condition in (B.4) is met. The step-function  $\eta'(T)$  is still defined for the original temperature set point in  $\{T_i\}$ . The optimized temperature set  $\{T'_i\}$  is then found by choosing the  $k$ -th temperature point  $T'_k$  such that

$$\int_{T'_1}^{T'_k} \eta'(T) dT = \frac{k}{M},$$

where  $1 < k < M$  and the two extremal temperatures  $T'_1 = T_1$  and  $T'_M = T_M$  remain fixed.

The feedback algorithm can be summarize by the following sequence of steps

1. Start with a trial temperature set  $\{T_i\}$ .
2. Repeat
  - (a) Reset the histograms  $n_{up}(T) = n_{down}(T) = 0$ .
  - (b) For the current temperature set perform a parallel tempering simulation with  $N_{SW}$  swap moves. After each sequence of swap moves, update the labels of all replicas. Record histograms  $n_{up}(T)$  and  $n_{down}(T)$ .
  - (c) For the given temperature set as estimate an optimized probability distribution  $\eta'(T)$  via

$$\eta'(T) = C' \sqrt{\frac{1}{\Delta T} \frac{df}{dT}}.$$

- (d) Obtain the optimized temperatures  $\{T'_i\}$  via

$$\int_{T_1}^{T'_k} \eta'(T) dT = \frac{k}{M}.$$

- (e) Increase the number of swaps  $N_{SW} \leftarrow 2N_{SW}$ .

3. Stop once the temperature set  $\{T_i\}$  has converged.

The initial number of swaps  $N_{SW}$  should be chosen large enough such that a few of round-trips are recorded, thereby ensuring that steady-state data for  $n_{up}(T)$  and  $n_{down}(T)$  are measured. The derivative  $df/dT$  can be determined by a linear regression, where the number of regression points is flexible. Initial batches with the limited statistics of only a few round trips may require a large number of regression points than subsequent batches with smaller round-trip times and better statistics.



ศูนย์วิทยทรัพยากร  
จุฬาลงกรณ์มหาวิทยาลัย



## VITAE

Mr. Luecha Tungchanachaiyanun was born on November 26, 1983 in Chonburi. He is the first child of Mr. Rungyot Tungchanachaiyanun and Mrs. Weena Tungchanachaiyanun. He received his B.Sc. degree in physics from Chulalongkorn University in 2006.



ศูนย์วิทยทรัพยากร  
จุฬาลงกรณ์มหาวิทยาลัย